analytical chemistry

Review

pubs.acs.org/ac

Chromatographic, Electrophoretic, and Mass Spectrometric Methods for the Analytical Characterization of Protein Biopharmaceuticals

Szabolcs Fekete,[†] Davy Guillarme,[†] Pat Sandra,[‡] and Koen Sandra*[,‡]

[†]School of Pharmaceutical Sciences, University of Geneva, University of Lausanne, Boulevard d'Yvoy 20, 1211 Geneva 4, Switzerland

[‡]Research Institute for Chromatography (RIC), President Kennedypark 26, 8500 Kortrijk, Belgium

CONTENTS

Protein Biopharmaceuticals 480
Chromatographic Approaches 482
Ion-Exchange Chromatography (IEX) 482
Size Exclusion Chromatography (SEC) 484
Hydrophobic Interaction Chromatography (HIC) 485
Hydrophilic Interaction Liquid Chromatography (HILIC) 486
Reversed Phase Liquid Chromatography (RPLC) 487
Electrophoretic Approaches 489
Capillary Zone Electrophoresis (CZE) 489
Capillary Isoelectric Focusing (cIEF) 492
Capillary Gel Electrophoresis (CGE) 493
Mass Spectrometric Approaches 494
Intact Protein and Middle-Up Measurements 495
Top-Down and Middle-Down Measurements 497
Bottom-Up Measurements 498
Glycan MS Measurements 502
Concluding Remarks 502
Author Information 502
Corresponding Author 502
Notes 502
Biographies 502
Acknowledgments 503
References 503

PROTEIN BIOPHARMACEUTICALS

Protein biopharmaceuticals are macromolecules with a therapeutic effect, commonly produced by the recombinant DNA technology. They have emerged as important therapeutics for the treatment of various diseases including cancer, cardiovascular diseases, diabetes, infection, inflammatory, and autoimmune disorders, etc.[1,2] Protein biopharmaceuticals come in many flavors and include monoclonal antibodies (mAbs), hormones, growth factors, fusion proteins, cytokines, therapeutic enzymes, blood factors, vaccines, and anticoagulants.[1,2] Given their obvious benefits in terms of safety and efficacy, these molecules have substantially reshaped the pharmaceutical market and close to 250 products, with 166 having distinct active ingredients, are approved for human use in the United States and the European Union.[1] With over 2 000 protein biopharmaceuticals currently in clinical development, the future of the biopharmaceutical market looks very bright. In 2013, protein biopharmaceuticals accounted for a total sales value of $140 billion representing approximately 20% of the total pharmaceutical market. Roughly 50% of that sales value is taken up by monoclonal antibodies which are being considered as the fastest growing class of therapeutics, with sales grown from $39 billion in 2008 to almost $75 billion in 2013, i.e., a 90% increase.[1−4] Sales of other protein biopharmaceuticals have only increased by 26% in the same time period, while small molecule drugs are stagnating.[4] In 2013, a total of 37 biopharmaceuticals (18 mAbs) displayed the status of blockbuster (sales >$1 billion) with the most lucrative product being adalimumab (Humira), generating global sales of $11 billion in 2013.[1]

The successes of mAbs have triggered the development of various next generation formats.[1,3,5] Since the approval of the first product in 1986, mAbs have already evolved from purely murine to chimeric to humanized to finally human, this to increase safety and efficacy. The mAb market is currently further reshaped by bispecific mAbs, antibody−drug conjugates (ADCs), antibody mixtures (polyclonal antibodies), antibody fragments (Fab, Nanobodies), Fc fusion proteins, and brain penetrant mAbs next to glyco-engineered formats.[1,3,5] In oncology, ADCs are particularly promising, since they synergistically combine a specific mAb linked to a biologically active cytotoxic drug via a stable linker.[6,7] The promise of ADCs is that highly toxic drugs can selectively be delivered to tumor cells thereby substantially lowering side effects as typically experienced with classical chemotherapy.[8] ADCs are expected to revolutionize cancer treatment and are bringing Paul Ehrlichs "magic bullet" concept to clinical reality.[9] Currently two ADCs are marketed, brentuximab vedotin (Adcetris) and ado-trastuzumab emtansine (Kadcyla) and over 30 are in clinical trials.[10,11]

With top-selling biopharmaceuticals evolving out of patent, recent years have also witnessed an eruption in activity around the development of biosimilars.[12−15] The biosimilar market holds great potential but is simultaneously confronted with huge challenges. In contrast to small molecule generics, which are synthesized by chemical means, exact copies of recombinant proteins cannot be made due to differences in the cell cloning and in the manufacturing process. Even originator companies experience lot-to-lot variation and often suffer with replicating their product after process changes.[16] As a consequence, regulatory agencies evaluate biosimilars based on their level of similarity with the originator, rather than the exact replication.[13] To date, 19 biosimilars have been approved in Europe including two mAb biosimilars (infliximab) which recently received marketing authorization.[1,17] The U.S. has been lagging

Special Issue: Fundamental and Applied Reviews in Analytical Chemistry 2016

Published: December 2, 2015

© 2015 American Chemical Society

DOI: 10.1021/acs.analchem.5b04561
Anal. Chem. 2016, 88, 480−507

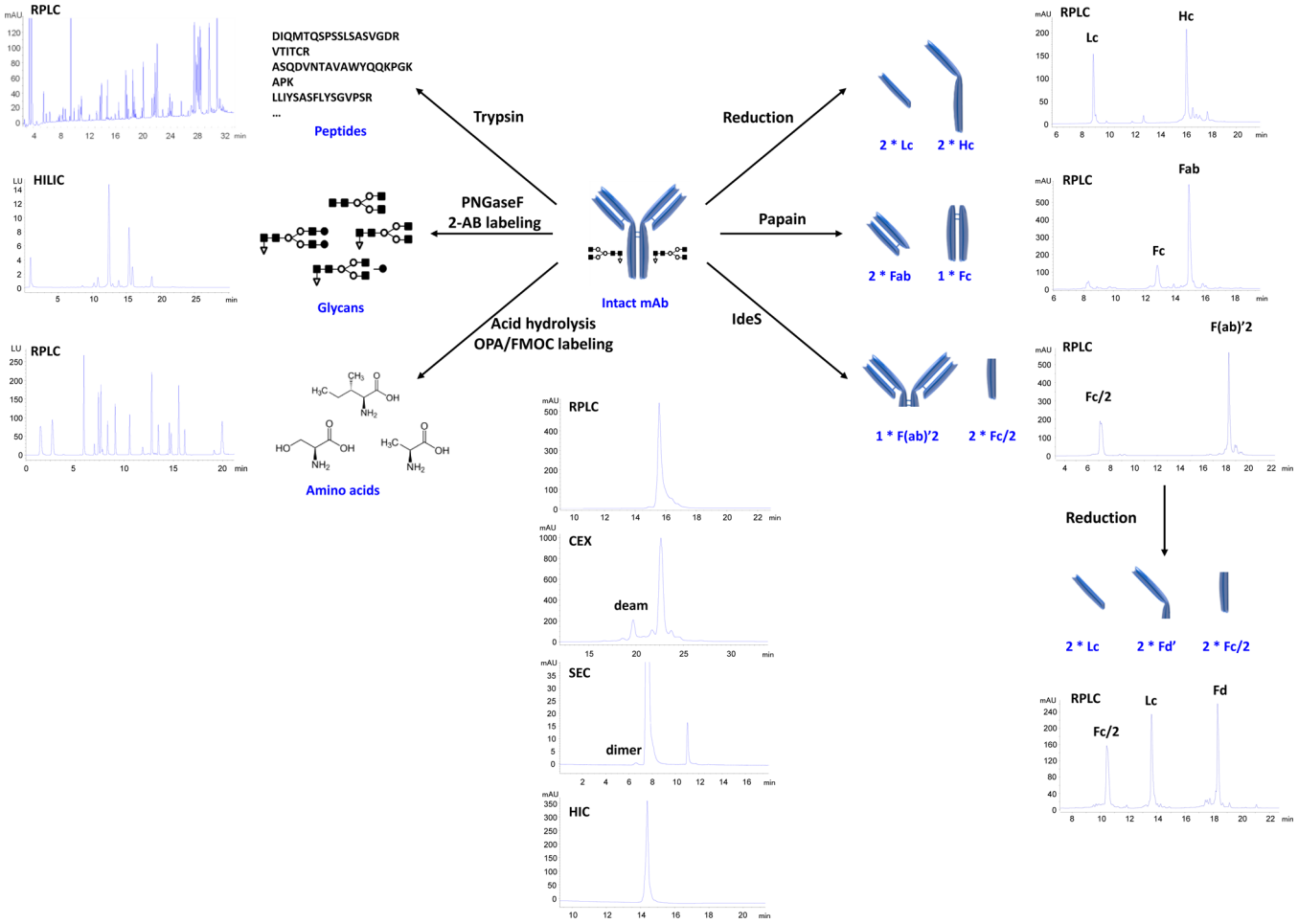


Figure 1. Summary of the different chromatographic approaches (RPLC, HIC, SEC, CEX, and HILIC) to characterize therapeutic mAbs (Herceptin as an example) at the protein, peptide, glycan, and amino acid levels. Apart for the glycans and amino acids chromatograms, which result from fluorescence detection, all data were acquired by UV.

behind, but with new regulation in effect, the first biosimilar was recently approved and this product is currently hitting the market.[18]

Protein biopharmaceuticals have a complexity far exceeding that of small molecule drugs. This can perfectly be illustrated when considering the structural aspects of a monoclonal antibody. mAbs are large tetrameric immunoglobulin G (IgG) molecules of approximately 150 kDa (±1 300 amino acids), forming Y-like shapes. They are structurally composed of four polypeptide chains, including two identical heavy chains (Hc) of ∼50 kDa and two light chains (Lc) of ∼25 kDa. These chains are connected through several inter- and intrachain disulfide bonds. From a functional point of view, mAbs consist of two regions, the crystallizable fragment (Fc) of ∼50 kDa, which is responsible for the effector function, i.e., antibody dependent cell-mediated cytotoxicity (ADCC) and complement dependent cytotoxicity (CDC) and the antigen binding fragment (Fab) of ∼50 kDa, which is primarily involved in antigen binding.[15,16,19,20] All mAbs are glycoproteins having two conserved N-glycosylation sites in the Fc region typically occupied with complex biantennary and high mannose type glycans. These glycan structures are known to play a role, among others, in the effector function and glyco-engineered mAbs with improved effector functions are currently being developed.[1,14,16] A variety of other chemical and enzymatic modifications (wanted and unwanted) taking place during expression, purification, and long-term storage further shape the mAb and give rise to a substantial heterogeneity.[16,20,21] Despite the fact that only a single molecule is cloned, thousands of possible variant combinations may exist for one given mAb and they all contribute to the safety and efficacy of the product. An informative overview of variants observed on mAbs, including glycosylation, asparagine deamidation, aspartate isomerization, succinimide formation, N-terminal pyroglutamate formation, C-terminal lysine truncation, oxidation, glycation, cysteine variants, sequence variants, etc. has recently been provided by Beck et al.[20] Liu et al. also provided a comprehensive overview of observed modifications and compared recombinant mAbs with endogenous IgG molecules secreted by B-cells.[21] It was concluded that modifications that are common to recombinant mAb and endogenous molecules are considered to pose a lower risk of immunogenicity, while modifications unique to the former could potentially pose higher risk. In comparison to naked mAbs, ADCs further add to the complexity because the heterogeneity of the initial antibody is superimposed with the variability associated with the conjugation strategy.[7,22,23] The ADC products are indeed often heterogeneous, with respect to drug loading and its distribution on the mAb. Next to the primary structure, mAbs also have distinct higher order structures dictating their function, which might be influenced by the above-described modifications, and can appear as dimers

DOI: 10.1021/acs.analchem.5b04561
Anal. Chem. 2016, 88, 480−507

or aggregates, which have the potential to induce immune responses.[16,20]

All these structural characteristics, together with their stabilities have to be revealed during development and subsequently need to be closely monitored prior to clinical or commercial release. In assessing these characteristics but also in demonstrating comparability, e.g., between originator and biosimilar, a significant number of analytical tools can be employed.[16,19,20,24] The present review provides insights into the chromatographic, electrophoretic, and mass spectrometric approaches reported in the last 2 to 3 years for the analysis of protein biopharmaceuticals, with a special focus on mAbs. From the overview provided here, it will become clear that characteristics such as amino acid sequence and composition, molecular weight and structural integrity, N- and O-glycosylation, N- and C-terminal processing, S−S bridges, free cysteine residues, deamidation (asparagine, glutamine), aspartate isomerization, oxidation (methionine, tryptophan), clipping, sequence variants, charge variants, aggregation, as well as higher order structural information can be extracted out of the generated data.

CHROMATOGRAPHIC APPROACHES

High-performance liquid chromatography (HPLC) is one of the key techniques for the characterization of biopharmaceuticals. Both LC hardware and software improved drastically in recent years and bioinert systems also appeared on the market. Today, LC systems can be operated at 1000 to 1500 bar, ultrahigh-pressure liquid chromatography (UHPLC), offering possibilities for either very fast or for high-resolution separations.[25] Column manufacturers have a wide range of stationary phase morphologies in their portfolio such as sub-2 μm fully porous, superficially porous particles, nonporous materials, as well as organic and inorganic monoliths and, moreover, dedicated biopharmaceutical columns were introduced. Among the different chromatographic modes, ion-exchange (IEX), size exclusion (SEC), hydrophobic interaction (HIC), hydrophilic interaction (HILIC), and reversed phase (RPLC) liquid chromatography are most often used for characterization of biopharmaceuticals.

As illustrated in Figure 1, the comprehensive characterization of protein biopharmaceuticals, e.g., mAbs, is typically performed at different levels being the protein, peptide, glycan, and amino acid level.[16] Because of the limited resolving power of different separation modes on intact proteins, partial enzymatic digestions and/or reduction of disulfide bonds are frequently used to ease the separation of smaller protein fragments. Pepsin, papain, or immunoglobulin-degrading enzyme of *Streptococcus pyogenes* (IdeS) are commonly employed to obtain relatively large fragments and simplify the investigation of their microheterogeneity.[26] Papain is used to generate Fc and Fab fragments of ∼50 kDa each, while pepsin and IdeS generate $F(ab')_2$ and Fc/2 fragments of, respectively, ∼100 and ∼25 kDa. The reduction of disulfide bonds can easily be performed by addition of strong reductive agents (e.g., dithiotreitol, DTT, or tris(2-carboxyethyl)phosphine, TCEP), to produce Lc and Hc fragments of, respectively, 25 and 50 kDa. Following IdeS digestion, further reduction generates three fragments of 25 kDa each, namely, Lc, Fc/2, and Fd. A next level of detail is obtained upon analyzing peptides which can be generated from the protein following their proteolytic digestion using enzymes like trypsin (cleavage next to arginine and lysine), chymotrypsin (preferably cleaves C-terminal of aromatic amino acids), AspN (cleavage N-terminal of aspartic acid), GluC (cleaves C-terminal of glutamic acid and aspartic acid), LysC (cleavage next to lysine), etc. In case information on S−S bridges is mandatory, digestion can be performed under nonreducing conditions, otherwise digestion is preceded by a reduction and alkylation step, e.g., using iodoacetamide to prevent the reformation of S−S bridges. A detailed characterization of glycans requires their removal from the protein backbone. N-glycans can be enzymatically liberated using "universal" endoglycosidases like PNGase F, PNGase A, Endo S, or Endo H. Since no universal O-glycosidase exists, O-glycans are commonly liberated by chemical means, e.g., β-elimination or hydrazinolysis. Amino acid compositional analysis requires the quantitative liberation of amino acids typically through acid hydrolysis at 110 °C for 24 h using 6 N HCl. In the following section, the different chromatographic modes and their applicability's will be illustrated.

Ion-Exchange Chromatography (IEX). Ion-exchange chromatography (IEX) is commonly used for profiling the charge heterogeneity of proteins resulting either from enzymatic or chemical modifications.[19,27] This separation mode is often employed both for characterization and release testing. Among the IEX modes, cation-exchange (CEX) is considered as the gold standard for the analysis of therapeutic proteins and two different elution modes are used. The first mode, the classical approach, involves an increase of the salt concentration during the gradient, resulting in weakening the ionic interactions, causing protein elution.[28] The second mode applies a pH gradient and therefore changes the protein charge and thus its interaction with the stationary phase.[29] Proteins are eluted in order of increasing binding charge (correlates more or less with the isoelectric point (p*I*) and equilibrium constant).

Regarding the stationary phases, ion-exchangers can be classified as either weak or strong exchangers. Weak cation-exchangers are comprised of a weak acid that gradually loses its charge as the pH decreases (e.g., carboxymethyl groups), while strong cation-exchangers are comprised of a strong acid that is able to sustain its charge over a wide pH range (e.g., sulfopropyl groups). In the case of proteins, the cation-exchange mode is well suited, but an anion-exchanger (AEX) can also be applied to bind the proteins if their p*I* is below pH 7.

Both silica and polymer based stationary phases are commercially available, in porous or nonporous format. For large proteins which possess low diffusivity, nonporous materials are clearly preferred to avoid some unwanted band broadening effects. State-of-the-art IEX columns are packed with 10, 5, or 3 μm nonporous particles, and a few sub-2 μm materials are also available. While the majority of IEX separations are performed on conventional (4.6 mm i.d.) or narrow-bore (2.1 mm i.d.) column formats, the use of capillary IEX has recently been demonstrated to achieve nanogram sensitivity of mAbs, which is particularly relevant in sample-limited applications, such as early stage candidate screening and *in vivo* studies.[30]

IEX has been shown to successfully resolve heterogeneities that might arise from modifications such as N-terminal cyclization (pyroglutamate formation), deamidation, C-terminal lysine truncation, sialylation, etc.[19,31,32] As example, Ganzler et al. developed a salt gradient based CEX method to compare different batches of biosimilar and originator mAbs (rituximab).[33] C-terminal lysine variants and also some acidic species were well separated within 18 min using a 100 mm × 4.6 mm column. The mobile phase pH was set to pH 6 with 2-(*N*-

DOI: 10.1021/acs.analchem.5b04561
Anal. Chem. 2016, 88, 480−507

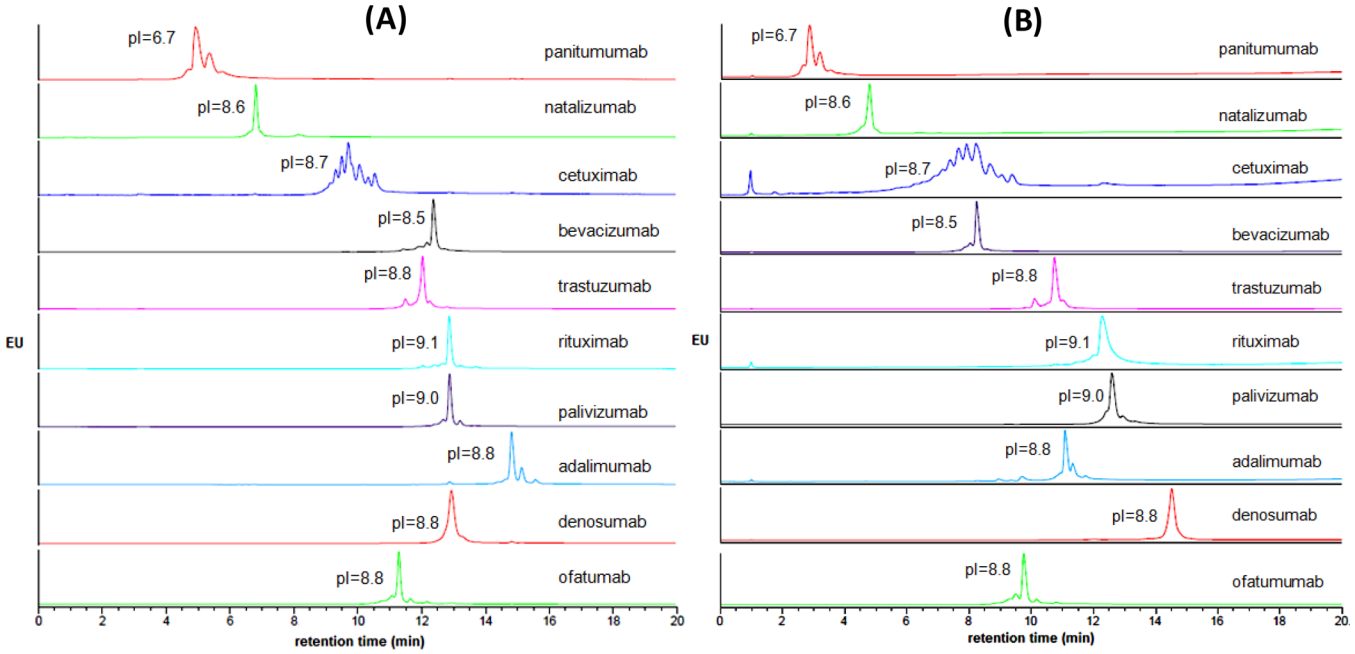


Figure 2. Generic salt (A) and pH (B) gradient CEX separation of different classes of mAbs. Multiproduct mAb separation is feasible in both elution modes. Reprinted from *J. Pharm. Biomed. Anal.*, Vol. *102*, S. Fekete, A. Beck, J. Fekete, D. Guillarme, Method development for the separation of monoclonal antibody charge variants in cation exchange chromatography, Part I: Salt gradient approach, pp 33−44 (ref 28). Copyright 2015, with permission from Elsevier; and from *J. Pharm. Biomed. Anal.*, Vol. *102*, S. Fekete, A. Beck, J. Fekete, D. Guillarme, Method development for the separation of monoclonal antibody charge variants in cation exchange chromatography, Part II: pH gradient approach, pp 282−289 (ref 29). Copyright 2015, with permission from Elsevier.

morpholino)ethanesulfonic acid (MES) buffer and a sodium chloride gradient from 0 to 0.2 M was applied. A very similar comparison was performed by Visser et al., who concluded that the sum of the basic peaks of the rituximab biosimilar was within the originator range, while the sum of the acidic peaks was found to be slightly below the rituximab originator range.[34] Pace et al. performed CEX on the Fab and Fc fragments to determine the deamidation dependence of mAbs on buffer type, pH and temperature.[35] IEX is also frequently used for the characterization of other antibody-related products (bispecific antibodies, polyclonal antibodies (pAbs) or Fc-fusion proteins).[36−38] Thiomabs are antibodies with an engineered unpaired cysteine residue on each heavy chain that can be used as intermediates to generate ADCs.[39] Multiple charge variant peaks were observed during CEX analysis of several thiomabs. This charge heterogeneity was due to cysteinylation and/or glutathionylation at the engineered and unpaired cysteines through disulfide bonds formed during the cell culture process.[39] When the conjugation is made through lysine amine residues of mAbs, ion-exchange chromatography (IEX) may be a valuable approach for resolving the different ADC species. Indeed, conjugation decreases the net positive charge of the mAb by one for each attached drug linker, if the drug linker is itself uncharged. No such separations have been reported in the literature up until now.

Very recently, Rathore et al. suggested performing nonlinear salt gradients to speed up the separation of mAb variants.[40] A detailed examination of nonlinear gradient shape has been performed by evaluating concave down, concave up, and sigmoidal shapes. Finally, a sigmoidal gradient shape has been proposed for the analysis of two mAbs and two salt types and was capable of performing the separation in less than 4 min. On the basis of this study, it seems that nonlinear gradients in IEX are promising, despite the fact that researchers are developing exclusively linear gradient systems, probably to limit issues when transferring IEX methods between different instruments.

Beside the classical salt gradient mode, the pH gradient mode is becoming more and more popular.[41−43] Kang et al. developed a two components buffer system for CEX pH gradient separation of mAb isoforms.[44] Several pH ranges were studied, and it was found that linear pH gradient was hardly feasible over a wide pH range. The developed system was appropriate to monitor the deamidation of various mAbs. Earlier on, a three component buffer system was proposed to perform a highly linear pH gradient. Systems made of Tris base, piperazine and imidazole enable developing linear pH gradients between pH 6 and 9.5.[45] Separation based on this three component buffer was validated for routine biopharmaceutical applications such as stability indicating methods.

In the past few years, vendors communicated that pH gradient is probably more generic than salt gradient because it enables to develop "multiproduct" methods. A head-to-head comparison was recently performed for salt and pH gradient based separations of several mAbs.[28,29] The impact of experimental parameters such as mobile phase pH, gradient steepness, and temperature on mAbs charge variants separation was studied. After optimizing the conditions, it was found that very similar separation (resolution and analysis time) can be achieved with the two modes. Similar selectivity was obtained, and slightly higher peak capacity was attained in the salt gradient mode for several mAbs. An important disadvantage was the cost and the limited number of providers offering buffer systems for pH gradients. Finally, both separation modes enabled to develop a "multi-mAb" separation of 10 mAbs possessing a p*I* between 6.7 and 9.1, more or less with the same efficiency and throughput. Figure 2 shows the chromatograms

DOI: 10.1021/acs.analchem.5b04561
Anal. Chem. 2016, 88, 480−507

obtained by the generic salt and pH gradient. Next to the separation of charge variants, pH gradient based IEX chromatography can also be applied to evaluate the p*I* of intact mAbs.[28,29]

Method development in IEX is often based on trial and error or "one-factor-at-a-time" (OFAT) approaches. Computer-assisted method development in other LC modes is quite common and was also recently applied in IEX mode. Because of the system nonlinearity, finding the optimum conditions is challenging. For salt gradient based separation, it seems that temperature is not a relevant parameter for tuning selectivity and should be kept at 30 °C, to achieve high resolving power (elevated peak capacity).[28] Because the relationship between apparent retention factors and gradient time can be described with a linear function, only two initial gradient runs with different slopes are required to fully optimize the salt gradient program. For pH, a second order polynomial model (i.e., based on three initial runs) is preferred to describe retention factor (k) vs pH dependence. When using an experimental design, it appeared that method optimization can be rapidly performed, in an automated way thanks to HPLC modeling software, using two gradient times and three mobile phase pHs. Such a procedure can be applied routinely and drastically decreases the time spent for method development. In the pH gradient mode, it was found that the retention of large proteins can be accurately modeled as a function of gradient steepness and mobile phase temperature.[29] Because the retention models were always linear, only four initial experiments (2 gradient times at 2 temperatures) were required to model the behavior in the CEX pH gradient.

IEX can also be combined with other chromatographic modes for two-dimensional (2D) separations. A very promising combination of chromatographic modes for protein analysis is IEX as the first and RPLC as the second dimension. In this configuration, it becomes possible to acquire mass spectrometric (MS) information from an IEX separation that is hardly feasible in regular IEX, except when using MS compatible mobile phases. A recent work illustrated the potential of online selective comprehensive 2D LC−MS (IEX × RP-MS) for direct identification of mAb isoforms and subunit analysis, through the case study of rituximab.[46] The combination of these two chromatographic modes allowed the direct assignment of the CEX peaks, using data from the time-of-flight-mass spectrometric (TOF-MS) detection. In addition, this 2D approach provides an improvement in peak capacity and resolution when high-performance second dimension separations are used, instead of simply using the second dimension separation as a desalting step. This was particularly relevant when separating rituximab fragments of medium size (25 kDa).

IEX finds applications beyond the separation of proteins. High-performance anion-exchange chromatography with pulsed amperometric detection (HPAEC-PAD) is commonly used to measure released N- and O-glycans as well as the monosaccharide building blocks without derivatization.[47,48] The method takes advantage of the weakly acidic nature of carbohydrates allowing separations at high pH using a strong AEX stationary phase. Glycans and monosaccharides are detected by measuring the electrical current generated by their oxidation at the surface of a gold electrode. In two recent studies, the capability of HPAEC-PAD in measuring mAb N-glycosylation was compared to orthogonal chromatographic and electrophoretic methods.[47,48] Both studies concluded that HPAEC-PAD is providing consistent and comparable results to the gold standard N-glycan analysis method based on HILIC and 2-AB labeling.

Size Exclusion Chromatography (SEC). Size exclusion chromatography (SEC) is historically widely used for the evaluation of protein aggregation and fragmentation.[19,27,49] The main advantage of SEC is the mild mobile phase conditions (ambient temperature in aqueous mobile phase at pH close to physiological conditions) that permit the characterization of proteins with minimal impact on the conformational structure and local environment. SEC is therefore considered as a nondenaturating mode.

In SEC, the separation is based on the hydrodynamic radius (size) of the proteins. The stationary phase consists of spherical porous particles with controlled pore size, through which the biomolecules diffuse based on their molecular size difference. In theory, a large volume and large porosity is required for SEC separations therefore typically 300 mm long and 7−8 mm i.d. columns have been used for routine separations. However, because of the numerous developments in column technology, now shorter (e.g., 15 cm) and narrower (4.6 mm i.d.) columns packed with smaller-sized particles (below 5 μm) are often applied to improve the throughput and resolution.

Two types of SEC packing are available: (1) silica (with or without surface modification) and (2) cross-linked polymeric packings.[50] The most common silica phases contain chemically bonded 1,2-propanediol groups that provide a hydrophilic (inert) surface. The latest generation of silica-related packings is an ethylene-bridged hybrid inorganic−organic (BEH) material that is currently available with sizes of 1.7 and 2.5 μm.[51] Very recently, a silica based 1.8 μm SEC material was also released. There have been a number of different hydrophilic packings developed for the SEC of biopolymers. Most of the cross-linked polymeric packings are proprietary hydroxylated derivatives of cross-linked polymethacrylates.[50]

By using sub-2 μm SEC columns (often termed as UHPSEC) in 150 mm × 4.6 mm dimensions, the analysis time can be shortened typically into the 3−5 min range.[51] However, using small particles packing can generate very high pressures. Therefore, thermal effects (frictional heating) and shearing forces might become critical for temperature or pressure sensitive proteins.[49] It was shown that elevated temperature and high pressure could induce on-column aggregation of an IgG1 mAb.[51] Moreover in many cases, UHPSEC and conventional SEC separations showed different results when quantifying mAb aggregates from the same sample.[51,52] So, applying UHPSEC is indeed useful to save time, but results have to be handled carefully. Using two SEC columns in parallel can also be a good way to improve throughput. Moreover, when combining interlaced sample injections and the parallelization of two narrow bore column, packed with sub-2 μm particles, it is possible to drastically shorten the analysis time. This parallel and interlaced SEC approach was described by Farnan et al. and applied for the fast determination of mAb aggregates.[53]

Several detection modes are currently applied for SEC. Ultraviolet spectrophotometry (UV) is still the predominant detection mode, but sensitivity and selectivity can be significantly improved with fluorescence detection.[49] The combination of multiple detectors including refractive index (RI), ultraviolet (UV), light scattering (LS), or multiangle light scattering (MALS), multiangle laser light scattering (MALLS), and viscometry (VM) allows extensive characterization of protein samples.[49] Using SEC-UV, Lu et al. observed a peak

DOI: 10.1021/acs.analchem.5b04561
Anal. Chem. 2016, 88, 480−507

(0.2−0.3%) eluting between mAb monomer and dimer peaks. The simultaneously acquired MALLS data suggested the peak to have a MW larger than the monomer but smaller than the dimer. Mass spectrometric analysis on the collected and desalted peak demonstrated two structural variants, a mAb with one extra light chain and a mAb with two extra light chains. These structural variants were shown to reduce potency by a factor of 2.[54] While several groups collect SEC peaks and analyze them via MS following desalting, there is a clear trend toward online SEC-MS. However, there are challenges to interfacing SEC with MS due to the inherent incompatibility of the mobile phases containing high concentrations of nonvolatile salts. To overcome this difficulty, SEC-MS methods have been developed using nondenaturing mobile phases containing volatile salts or denaturing mobile phases containing organic solvents and ion-pairing reagents instead of large amounts of nonvolatile salts.[55] As example, a high-throughput method was developed by Latypov et al. to differentiate candidate recombinant human monoclonal IgG1 and IgG2 antibodies based on their propensity to form aggregates when subjected to agitation stress.[56] Intact mAbs were separated from soluble and insoluble aggregates using a SEC column packed with 1.7 μm particles. The components were identified with a UHPLC−TOF-MS platform and quantified by using unstressed control. Treatment of the antibodies with IdeS enzyme reduced sample complexity. A volatile ammonium acetate salt was used to generate MS compatible mobile phase matching the pH formulation. Also 5% acetonitrile was added to improve MS sensitivity. Valliere-Douglas et al. also demonstrated the benefit of native SEC-MS for the determination of the intact mass of antibodies conjugated with small molecule drugs at interchain cysteine residues.[57]

To improve the sensitivity of aggregate detection or to work with very small amounts of available samples, the use of capillary columns in SEC is a valuable approach. However, several modifications are required to conventional HPLC systems to reduce the system volume and associated extra-column band broadening, which could be critical for routine applications. Until now, the number of publications in this field is rather limited, but 300 mm × 300 μm i.d. SEC capillary columns were successfully applied for the separation of mAbs fragments.[58,59]

Finally, SEC has also been employed for ADC characterization, but regular SEC conditions often provide poor peak shapes of ADCs and unacceptable resolution between aggregates and monomeric ADC products. This can probably be explained by the nonspecific interactions between the hydrophobic cytotoxic drugs and the surface of the stationary phase. To solve this issue, different organic modifiers can be added to the SEC mobile phase, such as isopropanol, acetonitrile, propylene glycol, or dimethyl sulfoxide.[22,49,60,61] In a recent study, SEC was coupled to RPLC in an online heart-cutting 2D chromatography format for identification and quantification of unconjugated small molecule drugs and related small molecule impurities in ADC samples.[61] The SEC column in the first dimension provided information on the size variants (dimers, aggregates) of the ADC and also separated the small molecular species from the ADC.

Hydrophobic Interaction Chromatography (HIC). Hydrophobic interaction chromatography (HIC) is historically a reference technique for the determination of the relative hydrophobicity of proteins and to achieve separation based on hydrophobic interactions between the protein and the stationary phase. In the past, HIC was widely applied on a preparative scale for protein purification, but today, it is more and more used at the analytical scale. The main advantage of HIC compared to other chromatographic modes is that it is a nondenaturating technique; therefore, the native forms (physiological-like) of the proteins are expected to be maintained and moreover the separated proteins can be collected for further activity measurements.[62] In HIC, the proteins are retained on a weak hydrophobic stationary phase (e.g., butyl) at high salt concentration (e.g., ammonium sulfate) and are eluted by decreasing the salt concentration (inverse gradient). This concept is based on the salting-out protein principle. The mobile phase is typically an aqueous solution of a nondenaturing (antichaotropic) salt such as ammonium sulfate and a buffer to control pH (usually phosphate, $6 \leq \text{pH} \leq 7$). The combination of a weakly hydrophobic packing with purely aqueous mobile phases minimizes protein denaturation and usually allows the recovery of native proteins from separated fractions. The retention in HIC is exclusively driven by the hydrophobic interaction between amino acid residues and the alkyl chain, or other nonpolar functional groups, bonded at the surface of the stationary phase. Therefore, the elution order in HIC enables to rank the proteins on the basis of their relative hydrophobicity.

Several developments were performed in HIC column technology to further improve the limited resolving power of this chromatographic mode.[63] Recent HIC stationary phases are generally prepared from nonporous particles, but there are also some porous polymethacrylate-based materials. HIC columns can be operated at pressures in the range 100−400 bar, and state-of-the-art columns are typically packed with 5, 3 and even 2.5 μm particles.[63]

Even if RPLC became dominant for analytical purposes due to the revolutionary improvements in RP column technology, the complementarity of the two modes is well understood and therefore HIC is regaining interest, especially for ADC characterization. HIC separates the different populations of intact ADC molecules that differ in the number of drugs per antibody which are called DAR (drug-to-antibody ratio) species.[64−66] Figure 3 shows a typical HIC elution profile of intact DARs of an IgG1 type cysteine linked ADC, which cannot be obtained in RPLC, due to the denaturating conditions. The drug-loaded species are resolved based on the increasing hydrophobicity, with the least hydrophobic,

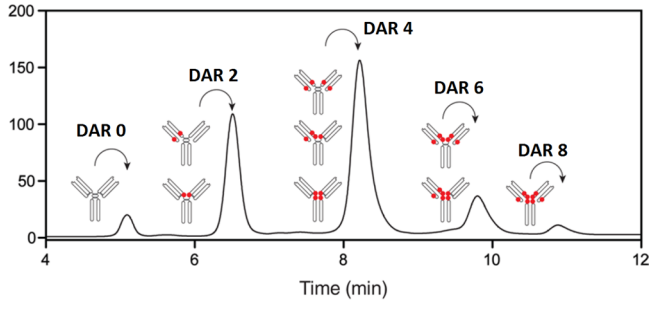


Figure 3. HIC elution profile of an IgG1 ADC showing the separation based on the number of conjugated drugs. Separation was performed by applying an inverse linear salt (ammonium sulfate) gradient on a butyl nonporous resin column. Reproduced from Le, L.N.; Moore, J.M.R.; Ouyang, J.; Chen, X.; Nguyen, M.D.H. Galush, W.J. *Anal. Chem.* **2012**, *84*, 7479−7486 (ref 66). Copyright 2014 American Chemical Society.

DOI: 10.1021/acs.analchem.5b04561
Anal. Chem. 2016, 88, 480−507

unconjugated form eluting first and the most hydrophobic, 8-drug form eluting last.[67] The relative distribution of the particular ADC species can be determined on the basis of peak area percentages. The weighted average DAR is then determined by using the percentage peak area information and the drug load numbers.[67] Several methods have recently been developed for the precise determination of DAR distribution of ADCs.[22,66] A mathematical approach using inputs from capillary gel electrophoresis (CGE) and HIC was developed to determine the positional isomer distribution within a population of ADCs.[66] The results were confirmed by analyzing isolated samples of specific DAR species. Debaene et al. applied HIC for off-line native MS characterization of an ADC, namely, brentuximab vedotin.[68] HIC fractions were collected and then analyzed by native MS and ion mobility (IM) MS, assessing the interpretation of each HIC peak. Next to measuring DAR, HIC has recently been used to highlight antibody heterogeneities originating from methionine and tryptophan oxidation, aspartate isomerization, succinimide formation, C-terminal lysine, and clipped species.[16] Using HIC, Ouellette et al. revealed a succinimide intermediate localized to an asparagine glycine motif in the heavy chain binding region of a mAb.[69]

HIC can also be a powerful strategy for multidimensional separations. The inherent problem of HIC is its incompatibility with MS detection. However, applying online multidimensional LC facilitates the combination of HIC and MS using a RPLC desalting step prior to MS. Birdsall et al. showed the potential of an online HIC-RPLC−MS setup for the characterization of isoforms of cysteine conjugated ADCs.[70] The ADCs dissociate into their respective subunits under the denaturing reversed phase conditions (mobile phase and temperature). This heart-cutting setup provided unambiguous identification of positional isomers and the drug conjugation site confirmation.

Hydrophilic Interaction Liquid Chromatography (HILIC). Hydrophilic interaction liquid chromatography (HILIC) is an important technique to analyze N-glycans originating from biopharmaceuticals.[16] Glycans are resolved on a polar stationary phase, commonly amide, by applying a water gradient thereby differentiating HILIC from normal phase LC (NPLC). Separation is based on the differential partitioning of the solutes between an acetonitrile-enriched mobile phase and a water-enriched solvent layer adsorbed onto the surface of the packing material. Electrostatic interactions also exist depending on the stationary phase, buffer, and pH. Combined with 2-aminobenzamide (2-AB) labeling and fluorescence detection, HILIC is nowadays the gold standard for glycan analysis and is performed on columns packed with sub-2 μm fully porous or sub-3 μm superficially porous particles.[16] Highly efficient separations of N-glycans including isomeric species as well as sialic acid and phosphate containing structures have been reported[16,71] and the method has extensively been used to assess comparability, e.g., between biosimilars and originators[34,72] or production batches.[73] In their comparison of different chromatographic, electrophoretic, and mass spectrometric technologies for N-glycan analysis, Reusch et al. used HILIC with 2-AB labeling as reference technology due to its wide acceptance.[47] The authors concluded from their study that all separation methods show excellent performance in terms of accuracy, precision, and separation and can be validated to be routinely used. They furthermore stress that the reference method used, namely, HILIC of 2-AB labeled N-glycans is best suited as a release tool. An et al. used this method to map the N-glycans on the receptor and Fc domains of a fusion protein following IdeS treatment and separation of both domains using Protein A purification.[74] Houel et al. recently performed an extensive N- and O-glycosylation analysis of the fusion protein Etanercept making use of an array of technologies.[75] The 2-AB labeled N-glycans were analyzed on HILIC as such or following their fractionation in neutral, monosialylated, and disialylated pools by weak anion-exchange (WAX) chromatography. Their identity was based on the retention time matches in glucose unit (GU) values combined with exoglycosidase digestion. Domain specific glycosylation information was obtained following RPLC fractionation of the TNF-α and Fc domains with subsequent HILIC analysis of PNGase F liberated and 2-AB labeled N-glycans. 2-AB labeled O-glycans, released using ammonia-based β-elimination, were as well analyzed using HILIC and their structures confirmed using exoglycosidase array digestions. The authors stated that 33.6% of the glycan structures observed were peeled artifacts resulting from the chemical release, illustrating the complexity associated with O-glycan analysis. Turyan et al. compared ammonia-based β-elimination to hydrazinolysis for the release of O-glycans. On the basis of the HILIC analysis of 2-AB labeled glycans, it could be concluded that hydrazine is 20−30 times more efficient in liberating O-glycans.[76] Ponniah et al. reported on the use of HILIC and 2-AB labeling for the quantification of low-abundance N-glycans.[77] These minor structures are highly relevant to the stability and function of mAbs. The detectability of low abundant peaks was increased by removing heterogeneity using an array of enzymes including EndoH, β-galactosidase, and β-*N*-acetylhexosaminidase.

In biopharmaceutical development, one is often confronted with high sample numbers benefiting from high-throughput glycan analysis workflows. In that respect, automated robotic platforms, incorporating mAb purification directly from cell culture media, N-glycan release, 2-AB labeling, and purification, have been described.[78,79] While reductive amination with 2-AB is well adapted in many laboratories, it has recently been challenged by novel reagents that either speed up the labeling or allow high sensitivity MS measurements.[80−82] Cook et al. redesigned the 2-AB labeling via reductive amination by instant AB labeling of the glycosylamine end of PNGase F liberated N-glycans.[80] In addition, the authors also sped up their deglycosylation procedure by immobilizing antibodies prior to PNGaseF treatment and their chromatography by down-scaling the particle diameter to sub-2 μm. As such, their entire N-glycan methodology was reduced from 3.5 days to 3.5 h. In the comparison of different N-glycan analysis approaches, Reusch et al. demonstrated that the HILIC method incorporating instant AB labeling is very comparable in performance (i.e., separation, precision, accuracy) to the reference 2-AB method.[47] In that particular study, the reference method was already optimized in terms of throughput and required 4 h of sample preparation compared to 2 h using the instant AB method. 2-AB labeling was also compared to procainamide labeling, proceeding via a reductive amination, and it was concluded that both show comparable glycan separation, but the latter gives higher fluorescence as well as 30-fold better electrospray ionization (ESI) efficiency, which can be explained by the high proton affinity of the procainamide basic tail. Deglycosylation, labeling and purification were fully automated on a liquid handling robot.[82]

Combining features of instant AB and procainamide, a new N-glycan labeling reagent was recently proposed, providing

DOI: 10.1021/acs.analchem.5b04561
Anal. Chem. 2016, 88, 480−507

enhanced fluorescence response and MS sensitivity. Moreover, this new labeling reagent rapidly reacts with glycosylamines upon their release from glycoproteins.[81] Within a 5 min reaction, N-glycans are labeled with this reagent comprised of an *N*-hydroxysuccinimide (NHS) carbamate reactive group, a quinoline fluorophore, and a tertiary amine for enhancing ESI ionization. The fluorescence and MS response factors of the labeled glycans were benchmarked to response factors for glycans labeled with 2-AB, instant AB, and procainamide. A 14-times higher fluorescence and a 160-times greater MS signal versus 2-AB labeled glycans were observed.

HILIC has less extensively been used for the separation of peptides and proteins. Clear benefits opposed to reversed phase HPLC peptide mapping have nevertheless been demonstrated for the separation of glycopeptides.[83,84] HILIC has also been used as the first dimension in LC × LC peptide mapping (HILIC × RPLC) of mAbs. It compared unfavorably to the combinations SCX × RPLC and RPLC × RPLC largely due to mobile phase incompatibilities.[85] More protein separations are expected on HILIC in the coming years with the recent introduction of widepore amide HILIC phases from various vendors.

Reversed Phase Liquid Chromatography (RPLC). The main benefits of RPLC over any other chromatographic mode are its high resolving power and inherent compatibility with MS.[19] The superior robustness of RPLC also makes it well suited for its use in a routine environment.[16] In RPLC, the solute retention is mainly mediated through hydrophobic interactions between the amino acid residues of the proteins and the bonded ligands of the stationary phase, similarly to HIC, but some secondary interactions (ion-exchange, H-bonding) always occur in RPLC. Moreover, the RPLC mobile phase is quite harsh compared to the HIC one. Indeed, routine RPLC analyses of proteins and derived products are commonly performed at 60−90 °C, with mobile phases containing acetonitrile, isopropanol, or methanol and trifluoroacetic acid (TFA) or formic acid (FA).

A first complication related to the analysis of biopharmaceuticals at the protein level in RPLC is their adsorption onto the stationary phase, that is especially critical for mAbs, due to some specific secondary interactions.[86,87] Two solutions are proposed to decrease the strength of secondary interactions and thus resolve adsorption issues. First, increasing mobile phase temperature up to 80−90 °C appeared as a promising solution. However, temperature should be used with caution as it can partially damage large proteins, e.g., cleavage in the hinge region of mAbs.[88] A compromise between residence time and temperature has to be found (typically shorter than 15 min). Second, it could be useful to add a small amount of an ancillary solvent, such as *n*-butanol to the mobile phase. Indeed, the hydroxyl group of *n*-butanol probably interacts with water adsorbed on the residual silanol groups "to shield" the silanols, thus limiting adsorption.[87] The above-discussed recovery issue is also less significant with antibody fragments compared to intact mAbs. Therefore, the 25 kDa fragments can be analyzed at lower temperature (e.g., 40−70 °C) without serious adsorption.

Second, proteins typically elute as broad peaks, due to their slow diffusivity and mass transfer resistance. The mass transfer resistance of large molecules is mostly accounted for by a slow external film mass transfer (mass transport across the boundary mobile phase layer of the particles).[89] It appears that the improvement in the column efficiency of large molecules should be related to the easier access of the molecules to the internal stationary phase volume. The use of UHPLC systems and columns packed with state-of-the-art very efficient widepore sub-2 μm fully porous or superficially porous (3−4 μm) particles opened new avenues for protein analysis.[19] Since then, several generations of superficially porous widepore materials and organic monoliths have been commercialized and allow to achieve very fast or high-resolution protein separations.[26] Today, the most popular stationary phases include sub-2 μm fully porous widepore (300 Å) materials available with C3, C4, C8, C18, and diphenyl chemistries and 3.4−3.6 μm widepore superficially porous particles bonded with C4, C8 and C18 phases. Some poly(styrene−divinylbenzene) organic monolithic columns, with a macropore size of approximately 1 μm (without mesopores) also showed promising results.[90]

RPLC has been used at the intact protein level or for the analysis of large protein fragments (Lc, Hc, Fab, Fc, F(ab′)$_2$, Fc/2, Fd) generated following enzymatic (papain, pepsin, IdeS) or chemical cleavage (DTT, TCEP).[91,74] The technique is often applied in the biopharmaceutical industry to evaluate identity, purity, stability, shelf life and also as a release test.[26] In general, oxidized, reduced, and deamidated forms, among many others, possessing different hydrophobicity compared to the native protein can be separated and quantified.[16,19,74,92,93]

The possibility to achieve very fast (1−2 min) or high-resolution UHPLC separations was demonstrated by using different column dimensions for the analysis of oxidized and reduced intact proteins.[94] It was shown that kinetic performance, retention capability, selectivity for closely related proteins, loading capacity, as well as recoveries were satisfactory using recent superficially porous and sub-2 μm fully porous stationary phases. Acceptable separation of a therapeutic protein (filgrastim, ∼19 kDa) and some of its degradants was performed in less than 1.5 min using a 50 mm long column. When coupling columns in series (300 mm), a peak capacity of >150 was obtained for the same sample. Another study demonstrated the gain in resolution upon transferring a conventional HPLC method, on a column packed with 5 μm particles, to a UHPLC method, using columns packed with sub-2 μm particles.[16] All the related compounds of a 30 kDa protein were better resolved on the sub-2 μm material, within a comparable analysis time. The importance of column coupling to improve peak capacity for 150 kDa intact monoclonal antibodies was also reported.[92] In this work, a 150 mm long column generated a peak capacity value of n_c = 62, while the 300 and 450 mm long columns provided n_c = 95 and n_c = 117, respectively. Columns packed with widepore 3.6 μm superficially porous particles showed significant gain in analysis time and peak capacity compared to fully porous materials for intact protein analysis.[96] The related impurities of intact Interferon α-2A were separated within 5 min, applying a 150 mm long column. In another recent study, the same column was used to separate a N-methionylated variant of Interferon α-2A in both drug substance and final product and analyze the variants in untreated, oxidized and slightly degraded samples.[97] Columns packed with 400 Å superficially porous particles of 3.4 μm were also reported to perform very high peak capacity separation for large intact proteins. The fast separations of an intact protein mixture as well as very high-resolution separations of mAbs and associated variants were shown.[98] The differences between several sub-2 μm C3, C4, C8, and diphenyl phases were recently studied by Liu et al. for the separation of antibody

DOI: 10.1021/acs.analchem.5b04561
Anal. Chem. 2016, 88, 480−507

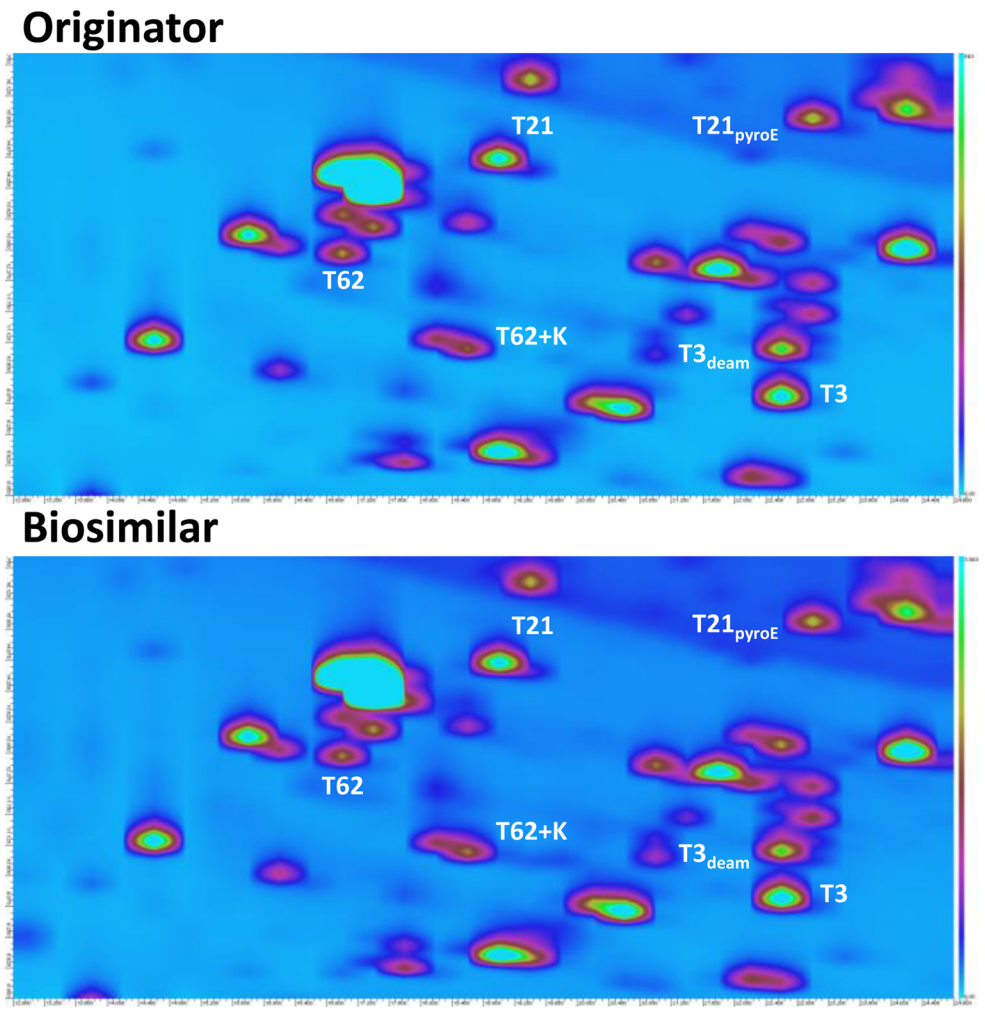


Figure 4. Detailed comparison of RPLC × RPLC peptide map (UV 214 nm) of a Herceptin originator and biosimilar in development. Impurities T62+K and T3deam are higher in the biosimilar. Impurity T21pyroE, associated with a pyroglutamate formation at the N-terminus of the heavy chain, is present in the same quantity in both the originator and biosimilar. With kind permission from Springer Science + Business Media: *Anal. Bioanal. Chem.*, Comprehensive two-dimensional liquid chromatography of therapeutic monoclonal antibody digests, Vol. *407*, **2015**, 355−366, Vanhoenacker, G.; Vandenheede, I.; David, F.; Sandra, P.; Sandra, K. Figure 2 (ref 85).

cysteine related variants.[99] The diphenyl phase was selected since it performed superior in terms of selectivity and recovery under the optimized conditions. MS detection was used to identify the different species.

RPLC has been shown to be the ideal second dimension technique in multidimensional separations of proteins. This is a direct result of its speed, efficiency, robustness, and compatibility with MS.[46,70] In combining IEX and HIC with RPLC, Stoll et al. and Birdsall et al. used, respectively, a widepore superficially porous C4 column and a widepore fully porous sub-2 μm C4 column.

A new superficially porous material made of a carbon core and nanodiamond-polymer shell was recently evaluated for the separation of therapeutic proteins.[100,101] The impact of pore size on the kinetic performance was studied and it was shown that pore size beyond 200 Å was required to achieve very efficient separations of large proteins. This material possesses a very small porous volume fraction compared to other superficially porous materials, since it is quite close to a nonporous particle structure. As the pore volume is decreasing, less impact of pore size is expected, but here with this unique particle structure, the pore size still played a role in the overall efficiency. It was also shown that a high TFA concentration of 0.3−0.5% was required when analyzing proteins, to achieve suitable peak shapes, but there was no need for elevated temperature to attain high peak capacities. This new material was finally applied for the analysis of real life samples of native, oxidatively stressed and reduced therapeutic proteins as well as reduced, digested mAbs and ADCs.[100]

Recently, an interesting alternative to superficially porous particles was proposed.[102,103] The so-called sphere-on-sphere (SOS) approach provides a simple and fast one-pot synthesis in which the thickness, porosity, and chemical substituent of the shell can be controlled by using the appropriate reagents and conditions.[104] SOS particles have been shown to be microporous with a pore diameter of less than 2 nm. However, while the surface of the material might not exhibit significant porosity, when packed into a HPLC column, the spaces between surface nanospheres provide superficial macroporosity. It has been proposed that for large molecules, larger pores as well as reduction of the shell thickness can be advantageous, due to the shorter diffusion distance and greater access to the surface area of the material.

DOI: 10.1021/acs.analchem.5b04561
Anal. Chem. 2016, 88, 480−507

Given its high resolution, robustness, and compatibility with MS, RPLC is also the method of choice to resolve peptides generated following proteolytic digestion of proteins using enzymes like trypsin, chymotrypsin, AspN, GluC, LysC, etc.[16] Peptide mapping is usually performed to confirm the primary structure, to assess modifications and modification sites and to demonstrate comparability.[16,34,71] By way of example, Sandra et al. described the peptide mapping of a 30 kDa recombinant therapeutic protein, validated for use in a routine environment for identity and purity testing.[16] The method achieved full sequence coverage at UV level and allowed to assess critical quality attributes, such as aspartate isomerization, at levels as low as 0.1% using UV 214 nm detection.

Peptide mapping is usually performed on columns packed with fully or superficially porous C18, C8, and C4 stationary phases using mobile phases containing water, acetonitrile, and 0.1% TFA or FA using a gradient evolving from low to high % of acetonitrile. This allows the elution of the very diverse peptides encountered in protein digests.[16,105,106] Optimal chromatographic separation is obtained when using TFA over FA, this at the expense of mass spectrometric sensitivity. As an alternative to the common silica and hybrid based materials, the so-called CSH (charged-surface hybrid) C18 phase showed greater peak capacities and a unique selectivity for peptide mapping.[107,108] Its performance was also seen to be less dependent on TFA ion pairing making it ideal for MS applications.[108]

Since protein digests can be very complex, peptide mapping demands for the best in terms of chromatographic separation. By coupling of columns, a peak capacity of more than 700 was achieved for mAb peptide mapping with a gradient time of 270 min and a column length of 450 mm.[95] Vanhoenacker et al. recently described the possibilities of using LC × LC as novel tool for peptide mapping of therapeutic mAbs (originators and biosimilars) in both R and D and routine (QA/QC) environments.[85] Compared to one-dimensional LC (1D-LC), LC × LC substantially increased resolution and was shown to be an attractive technique for identity, purity, and comparability assessment. Several LC modes were combined, i.e., SCX × RPLC, HILIC × RPLC, and RPLC × RPLC. The latter, performed at pH extremes, was surprisingly powerful and the partial correlation was overruled by the high peak capacity in both dimensions (RPLC has a higher peak capacity than SCX and HILIC). Moreover, RPLC × RPLC is very robust because of the solvent compatibility and can form the basis for the development of robust generic QA/QC methods in the pharmaceutical industry. The use of RPLC × RPLC in comparability assessment of a Herceptin originator and biosimilar in development is shown in Figure 4.

As an orthogonal method to HILIC, RPLC has as well been used to separate glycans following their removal from the protein backbone and their labeling with hydrophobic tags such as 2-aminobenzamide (2-AB) and 2-aminobenzoic acid (2-AA). The selectivity of RPLC in combination with 2-AA labeling enables the separation of a variety of structural isomers of different types of N-glycans and, more important, separates the N-glycans into seven different groups: oligomannose, hybrid and complex without core fucosylation, hybrid and complex with core fucosylation, and two sialic acid-containing groups again with and without the core fucose residues.[109] Porous graphitic carbon as stationary phase is also used for glycan analysis.[110−114] The chemical nature and physical structure of the graphite allow unique retention and separation of polar compounds. Solvents and additives used for elution from graphitic columns are similar to those used in classical RPLC; many are mass spectrometry compatible. Song et al. and Oh et al. described the analysis of, respectively, underivatized mAb and erythropoietin N-glycans using a porous graphitized carbon column incorporated in a chip.[113,114] Reusch et al. compared porous graphitized carbon chromatography with MS detection to the gold standard N-glycan analysis method based on HILIC and 2-AB labeling. Consistent results in terms of precision and accuracy were obtained.[111] A porous graphitized carbon column has also been used in the second dimension separation of 2-AA labeled fusion protein N-glycans fractionated by mixed mode HILIC and AEX.[112] Another study described a quantitative isomer-specific N-glycan fingerprinting method using isotope coded $^{12}C_6/^{13}C_6$ aniline labeling and LC−MS with a graphitic carbon stationary phase.[110] The validated method was used to compare the glycosylation in human mAbs produced in CHO and hybridoma cell lines. Graphitized carbon columns have also been used to analyze underivatized O-linked glycans released by reductive β-elimination.[115] Both neutral and acidic O-glycans containing sialic acid, hexuronic acid, and sulfate were successfully measured.

RPLC is furthermore the method of choice to separate amino acids after their liberation from proteins. Amino acid analysis is still extensively used to accurately quantify a protein biopharmaceutical and to determine the amino acid composition. Methods are mature and typically involve precolumn derivatization using o-phtaldialdehyde (OPA) for primary amino acids and 9-fluorenylmethyl chloroformate (FMOC) for secondary amino acids (proline) followed by separation and UV or fluorescence detection.[16]

■ ELECTROPHORETIC APPROACHES

Because of its high resolving power and miniaturized format, capillary electrophoresis (CE) has been widely applied for the analysis of biopharmaceuticals. In the different electrophoretic modes that can be employed, a high electrical field is always applied to separate molecules based on differences in charge, size, or hydrophobic properties.

Capillary Zone Electrophoresis (CZE). Capillary zone electrophoresis (CZE) is a technique perfectly adapted for the separation of proteins with post-translational modifications (PTMs) or degradations that affect the charge of the molecules, such as deamidation, sialylation, C-terminal lysine truncation, or N-terminal pyroglutamate formation. CZE, as a charged-based separation technique, is used to confirm the identity of a therapeutic protein, detect impurities, and characterize its charge heterogeneity.[115] Because the molecular weights of the protein variants are of comparable size, the separation selectivity in CZE is predominantly governed by charge differences.[116]

When analyzing large proteins on a bare fused-silica capillary, it is however important to keep in mind that adsorption of proteins at the surface of the capillary wall could be a severe issue. Indeed, the positive charges at the surface of the proteins (mAbs have relatively high p*I* values, in the range 7.5−9.5) will tend to interact with the negatively charged silanols at the capillary surface, through strong ionic interactions. This adsorption phenomenon usually prevents CZE from obtaining high plate counts. It also affects electro-osmotic flow (EOF) and analyte migration and could contribute to peak distortion. Various approaches were reported to reduce (but never completely eliminate) protein adsorption by either modifying

DOI: 10.1021/acs.analchem.5b04561
Anal. Chem. 2016, 88, 480−507

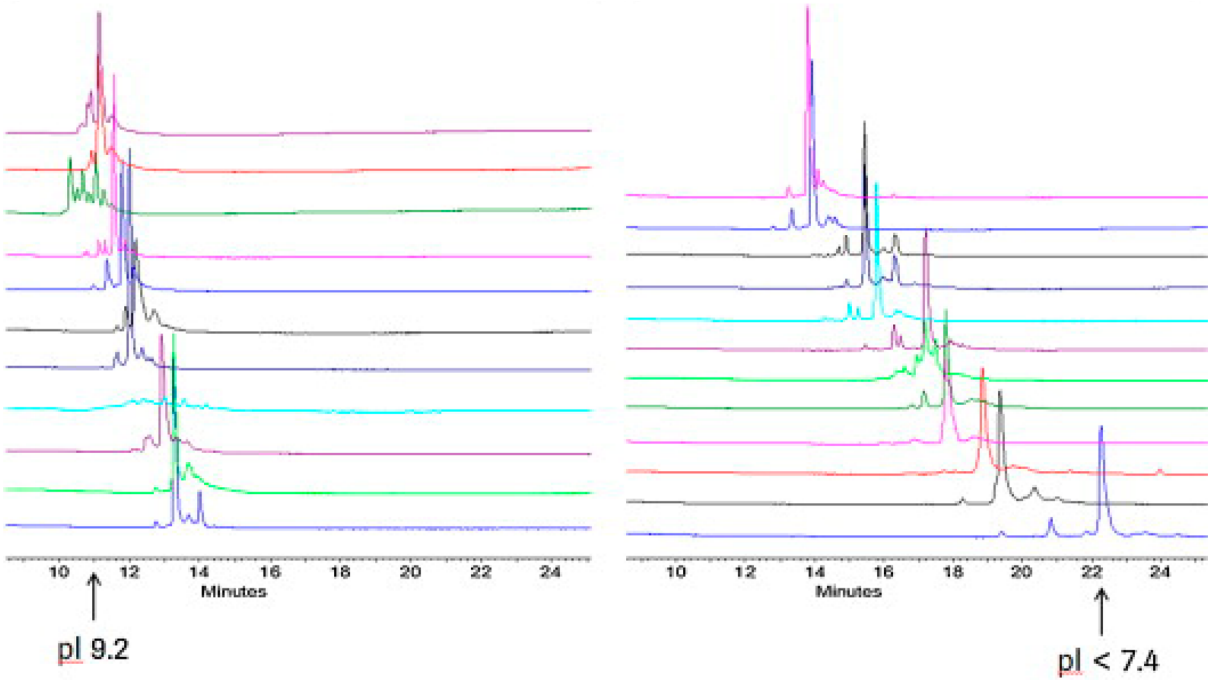


Figure 5. CZE separation of 23 mAbs with p*I* values ranging between 7.4 and 9.2. Separations were performed in a 50 cm capillary with an inner diameter of 50 μm. Reprinted from *J. Chromatogr. B*, Vol. *983*, Moritz, B.; Schnaible, V.; Kiessig, S.; Heyne, A.; Wild, M.; Finkler, C.; Christians, S.; Mueller, K.; Zhang, L.; Furuya, K.; Hassel, M.; Hamm, M.; Rustandi, R.; He, Y.; Salas Solano, O.; Whitmore, C.; Ae Park, S.; Hansen, D.; Santos, M.; Lies, M., Evaluation of capillary zone electrophoresis for charge heterogeneity testing of monoclonal antibodies, pp 101−110 (ref 125). Copyright 2015, with permission from Elsevier.

the density of charge on the protein or on the capillary wall. A first solution consists in tuning the pH or ionic strength of the background electrolyte (BGE).[117] Alternatively, it is also possible to add a modifier, such as surfactants, small amines, or anionic salts, to the BGE, in order to reduce the proteins−wall interactions. The last solution consists in using a dynamic or static capillary coating procedure to shield the protein from the fused-silica wall. Coating materials are generally classified as being charged (positively or negatively charged), to suppress ionic interactions; or neutral, to cover the silanol groups. Dynamic coatings are buffer additives that adsorb to the capillary surface and are quite popular, due to their ease of use and versatility, but regular regeneration is mandatory.[118] Despite some obvious advantages, dynamic coating is not the best option for reducing protein adsorption since it makes the approach incompatible with MS and, moreover, band broadening could also occur due to high separation current and Joule heating. Alternatively, static coatings are chemically linked to the capillary wall and represent a better technical solution, in spite of a non-negligible cost. Various companies have commercialized coated capillaries for protein separations. Gassner et al. have carried out a thorough study of various neutral and positively charged static coating solutions.[119] One of the most important conclusions of their study was that there were still some sites for protein adsorption on all neutral coated capillaries. Therefore, the separation performance achieved on all these coated capillaries was highly dependent on the composition and pH of the running BGE and there is a need to optimize concomitantly the BGE nature and coating. More recently, Ramsey et al.[120] performed a chemical vapor deposition of aminopropyl silane for coating microfluidic CE devices. The method was found to be simple, fast, reproducible, and reliable. With this coating approach, a strong anodic EOF was monitored and exceptional electrophoretic separation efficiency of between 100 000 and 400 000 plates for peptides and proteins analysis were monitored. The microfluidic device with an integrated ESI emitter was employed for the separation and characterization of mAb and mAb conjugate variants.[121] The separation of the charged variants facilitated their identification through MS detection. Except adsorption of proteins onto the inner wall of the capillary, another important constraint of CZE is the poor detection limit and thus sensitivity. CZE of proteins is generally carried out with UV detection at 214 nm, which is a universal absorption wavelength for peptide bonds, but the sensitivity is limited due to the short optical path length, limited injection volume, and the narrow internal diameter of the capillary. For improving sensitivity, two different approaches can be employed.[122] The first one consists in applying sensitive detectors such as laser-induced fluorescence (LIF) or MS. For MS, it is important to use a volatile BGE buffer, which is a constraint, as it is always hard to obtain narrow, sharp peaks of proteins in CZE, under such conditions. Biacchi et al. recently reported on the characterization of cetuximab variants implementing an off-line CZE-ESI-MS approach making use of fraction collection.[123] Alternatively, preconcentration techniques, such as stacking (the sample conductivity is less than that of BGE) or isotachophoresis (ITP) (the proteins will be concentrated between two electrolytes owing to different mobilities) can also be useful to improve limits of detection.

There are a significant number of papers reporting the use of CZE for separating charge variants of proteins.[123−127] Some consensus conditions were found for the analysis of mAbs. The buffer pH should be comprised between 4.5 and 6.0 and it is important to keep in mind that pH plays a major role for tuning selectivity of charge variants. Some additives also have to be

DOI: 10.1021/acs.analchem.5b04561
Anal. Chem. 2016, 88, 480−507

added to the running BGE to modify selectivity and/or reduce adsorption. As an example, the use of an ampholytic compound such as ε-aminocaproic acid (EACA) was found to decrease adsorption compared to ammonium acetate. A generic CZE method was recently applied to the analysis of 23 mAbs, with p*I* ranging from 7.4 to 9.2 within a total analysis time of 22 min (Figure 5).[125] In the described study, the performance of CZE was found to be superior to that of IEX and capillary isoelectric focusing (cIEF), and the precision as well as accuracy of the method were excellent (around 1% and 100%, respectively). An interlaboratory CZE study on stressed and nonstressed mAb samples was performed in 11 pharmaceutical laboratories. Since no significant differences were observed between the peak profiles, the reliability of CZE as a charge heterogeneity quality control method for mAb testing was clearly demonstrated. In addition, the interlaboratory study delivered precise results (standard deviations were in the range of 1%), without training of the participants prior to the study. In another work,[127] the authors demonstrated the possibility to use CZE-UV as a useful method to assess the comparability between mAb originators (i.e., rituximab and infliximab) and their biosimilar versions. With values less than 2% and 1%, the RSD of the isoform content and migration times were found to be excellent. However, the amount of information generated by these experiments is far too limited to conclude about the quality of a biosimilar and several other orthogonal techniques have to be employed concomitantly. Microfluidic chip zone electrophoresis was also developed to speed up (by a factor of 8 to 90-times) the determination of mAbs charge variants.[128] This allows the fast evaluation of quality in process development of biopharmaceuticals. Today, such microchip systems are commercially available for charge variant analysis and furthermore allow sizing and glycan measurements.

CZE was also employed for characterizing mAbs at the peptide level.[129] Here, CZE offers the advantage of providing alternative selectivity to RPLC and of separating both hydrophilic peptides that are generally eluting in the dead volume in RPLC and the largest peptides that could adsorb at the surface of the RPLC stationary phase.[130] While RPLC is still the preferred technology for peptide mapping, an interlaboratory study, involving 13 independent laboratories, recently demonstrated the robustness of CZE−MS for peptide mapping.[131] In the most recent works, the sheathless interface seems to be preferred over the well-established sheath flow CZE−MS interface. Gahoual et al.[132,133] reported the characterization of the primary structure and microvariants of several therapeutic mAbs in a single injection, after tryptic digestion, using sheathless CZE and MS. To attain sufficient sensitivity, transient isotachophoresis (ITP) was introduced as an electrokinetically based preconcentration technique allowing one to inject about 25% of the capillary length. The replacement of regular CZE−MS with ITP-MS offers the same interest as replacing LC−MS with nanoLC−MS. The full amino acid sequence was covered for four different mAbs including cetuximab and trastuzumab. In addition, PTMs, such as glycosylation, asparagine deamidation, and aspartic acid isomerization, were highlighted. The authors concluded that sheathless CZE−MS may be a suitable alternative to the widely adopted LC−MS approach. Very similar results on trastuzumab were recently reported by an independent research group.[134] Gahoual et al. also demonstrated the possibility to use CZE−MS as an efficient tool for assessing the comparability between cetuximab originator and a biosimilar candidate.[135] Full sequence coverage was obtained for both samples, and a difference of one amino acid was demonstrated between the two sequences. Characterization of glycoforms and hot-spot PTMs further demonstrated the poor quality of the biosimilar product compared to the originator. In another work, Biacchi et al. coupled CZE−UV to matrix-assisted laser desorption ionization (MALDI) MS allowing the characterization of the charge variants of a commercial mAb at the peptide level.[136] The complementarity of LC and CZE was demonstrated with the development of a hybrid multidimensional separation system made by coupling capillary LC to a microfluidic device integrating flow splitting, CZE, electroosmotic pumping, and ESI emitter elements.[137] This setup was employed for comprehensive online LC−CZE−MS of proteolytic digests of mAbs and generated a peak capacity of approximately 1400 in 50 min. This setup was also employed for characterizing the N-linked glycosylation of mAbs. The separation of a digested IgG2 containing two N-linked glycosylation sites is shown in Figure 6. The figure clearly illustrates the high degree of

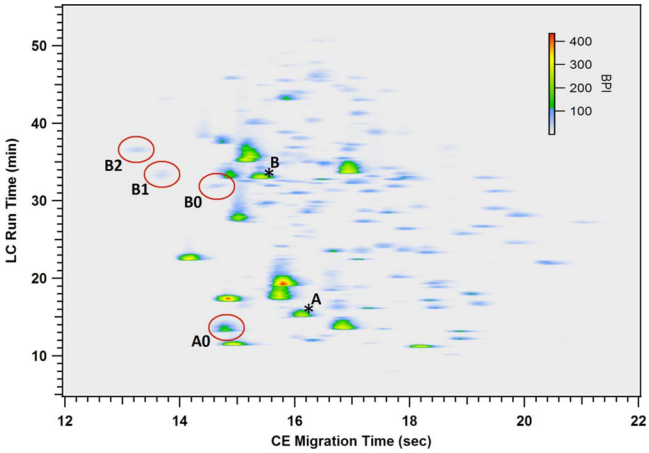


Figure 6. Image plot for the LC−CZE−MS separation of a digested IgG2 containing two N-linked glycosylation sites. The circled spots contain all of the observed N-linked glycopeptides. The spot labeled A0 contains all of the glycopeptides from the Fc domain site. Spots B0, B1, and B2 contain the glycopeptides from the Fab domain site containing 0, 1, and 2 sialic acid residues, respectively. The positions of corresponding unglycosylated peptides from each site are indicated with asterisks (*). Reproduced from Mellors, J. S.; Black, W. A.; Chambers, A. G.; Starkey, J. A.; Lacher, N. A.; Ramsey, J. M. *Anal. Chem.* **2013**, *85*, 4100−4106 (ref 137). Copyright 2013 American Chemical Society.

complementary/orthogonality of RPLC with a C18 material (first dimension) and CZE in the presence of 50% ACN (second dimension).

Finally, CZE has also been widely used to separate both labeled and unlabeled N-glycans. Compared to capillary gel electrophoresis (CGE), which is in widespread use for routine glycan analysis, CZE buffers are typically MS-friendly. Bunz et al. described a CZE−MS method for the analysis of native and 1-aminopyrene-3,6,8-trisulfonic acid (APTS) labeled N-glycans using a volatile alkaline BGE.[138] In order to generate an analogous separation compared to CGE-LIF of APTS labeled N-glycans, they subsequently re-evaluated their CZE−MS methodology and evolved to a strategy allowing to assign identities to CGE-LIF peaks.[139] It was concluded that glycan mobility databases may enable the assignment of peaks identified by CZE−MS to CGE-LIF peaks. Compared to LIF,

DOI: 10.1021/acs.analchem.5b04561
Anal. Chem. 2016, 88, 480−507

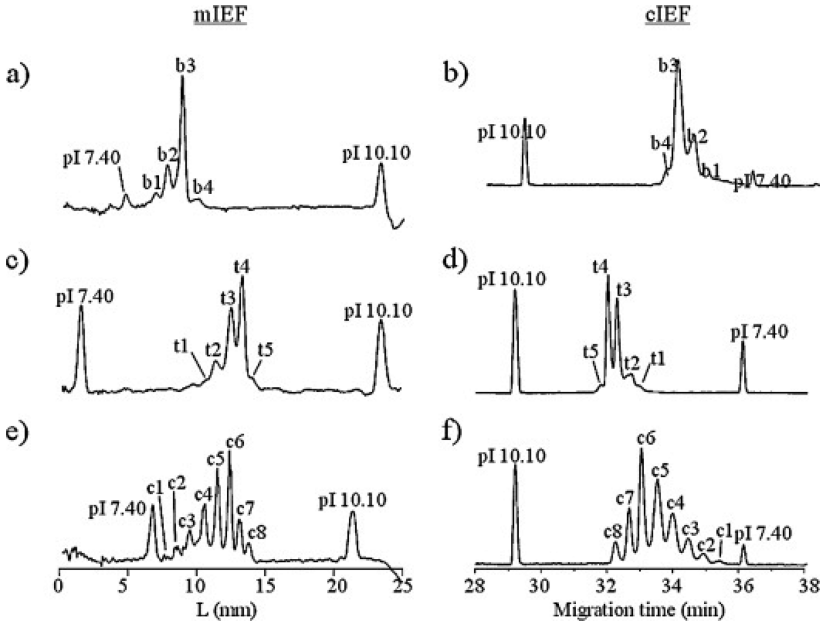


Figure 7. Analysis of charge variants of bevacizumab, trastuzumab, and cetuximab by mIEF (left column) and cIEF (right column). Peaks observed in each sample were labeled with numbers depending on their detection positions. Peak 1 means the most acidic-end peak. Reprinted from *J. Chromatogr. A*, Vol. *1309*, Kinoshita, M.; Nakatsuji, Y.; Suzuki, S.; Hayakawa, T.; Kakehi, K., Quality assurance of monoclonal antibody pharmaceuticals based on their charge variants using microchip isoelectric focusing method, pp 76−83 (ref 154). Copyright 2013, with permission from Elsevier.

MS is not offering the same sensitivity. To increase the sensitivity of glycan detection in CZE, it is possible to prepare the sample in a less conductive solution (stacking procedure), since analyte ions from the sample become concentrated on the sample/electrolyte interface.[140] In-line solid phase extraction (SPE)-CZE−MS has as well been described for APTS-labeled glycans and an enrichment factor of 800 was demonstrated.[141] Jayo et al.[142] proposed a flow-through microvial device to interface CZE and MS, for profiling both neutral and sialylated glycans without labeling. In this work, the CZE separation was carried out at near zero EOF in a capillary containing a neutral, hydrophilic coating. N-glycans derived from IgG and recombinant human erythropoietin (rHuEPO) were analyzed. Although baseline separation in the time dimension was not achieved for all the glycans, the MS provided complementary information and allowed direct analysis of underivatized neutral and acidic glycans in a single run. A total of 22 mAb N-glycans, including neutral and sialylated species, were identified. The presence of more than 70 N-glycans including O-acetylation, Neu5Ac/Neu5Gc heterogeneity, and extension of the glycan chains due to LacNAc repeats was revealed in rHuEPO. The authors furthermore state that the analysis of underivatized glycans maintains labile functionalities such as sialic acid and acetyl residues. This work clearly demonstrates the potential of CZE−MS to provide a comprehensive glycosylation profile and to evaluate the quality of biosimilar products.

Capillary Isoelectric Focusing (cIEF). Capillary isoelectric focusing (cIEF) is the adaptation of the traditional slab gel electrophoresis into the capillary format. Compared to the slab gel version, cIEF offers faster analysis times, higher resolution, and lower limits of detection. cIEF allows the separation of proteins based on their p*I*, in a pH gradient generated between the cathode and anode, thanks to the use of ampholytes mixed with the sample to establish the pH gradient. UV detection at 280 nm is generally used in cIEF, because the ampholytes exhibit strong absorbance at lower wavelengths. When the proteins are focused into highly concentrated bands at their p*I*, with a zero net charge, precipitation can occur. This can cause capillary clogging or irreproducible results. To avoid such issues, and enhance protein solubility, urea, sucrose, or a mixture of both have to be added to the sample. In the above-described approach, the proteins are first focused at the position where pH is equal to p*I* and then forced to move toward UV using a mobilization step. Because the mobilization tends to broaden peaks and increase analysis time, imaged cIEF (icIEF) has become the standard for protein analysis and allow to achieve faster separation, higher resolution, as well as better reproducibility, thanks to the whole column imaging technology within a transparent capillary.[143,144] The throughput of icIEF is also enhanced compared to cIEF, due to the use of very short capillary (only 5 cm length) and no need for the mobilization step.[145]

Similarly to what can be done in CZE, cIEF and icIEF are well suited for the characterization of charge heterogeneity.[74,146] Salas-Solano et al. recently demonstrated the possibility to use cIEF[147] and imaged cIEF[148] for the quality control of therapeutic proteins. For this purpose, they have performed two interlaboratory studies involving 12 laboratories from independent pharmaceutical companies. Both cIEF and icIEF possessed enough robustness and precision to be applied as a reliable quality control method for the charge heterogeneity of mAbs. A recent study also demonstrated the possibility to successfully validate a cIEF method for mAbs, according to ICH guidelines Q2(R1).[149] RSD values for isoelectric points and migration times were below 0.2% and 4%, respectively. Vanam et al. showed that the charge heterogeneity of chromatographically isolated antibody fragments (heavy and light chains) can be resolved using analytical SEC followed by icIEF, with a significant increase in throughput compared to 2D-PAGE.[150] Shimura et al. used ciEF to determine the

DOI: 10.1021/acs.analchem.5b04561
Anal. Chem. 2016, 88, 480−507

asparagine deamidation rates of a mouse IgG1 Fab.[151] Five asparagine residues were mutated one by one through site-directed mutagenesis, and the deamidation rates of the original Fab and the mutants were determined using ciEF.

Because of the presence of nonvolatile ampholytes, combining cIEF and ESI-MS is not easy. Some attempts have nevertheless been made and different strategies have recently been reviewed by Hühner et al.[152] Peaks observed via icIEF can typically not be characterized further by MS or other orthogonal methods. Dada et al. recently described the detailed characterization of both the acidic and basic regions of icIEF profile of an IgG1 antibody via preparative immobilized pH gradient IEF (IPG-IEF) fractionation.[153] Deamidation, sialylation, glycation, and fragmentation were identified as the main modifications contributing to acidic variants of the mAb, while C-terminal lysine, C-terminal proline amidation, and uncyclized N-terminal glutamine were the major species contributing to the basic variants.

To assess the heterogeneity of mAbs more easily and in a rapid manner, a commercially available microchip icIEF (mIEF) was evaluated and compared to regular cIEF.[154] As shown in Figure 7, the electrophoretic profiles of three commercial mAbs, namely, bevacizumab, trastuzumab, and cetuximab were consistent between the mIEF and the cIEF. The analysis time was reduced by 10-fold, while the repeatability in terms of calculated p*I* values and percent relative amounts of each charge variants were excellent on the mIEF. Despite these promising results, the authors concluded that there are still some improvements in terms of automation and sensitivity that should be brought to the mIEF setup, before widespread use in the pharmaceutical industry.

Capillary Gel Electrophoresis (CGE). Sodium dodecyl sulfate-polyacrylamide gel electrophoresis (SDS-PAGE) has been used for several decades for size-based separation of proteins. When SDS completely reacts with proteins, the reaction produces SDS−protein complexes of the same charge. Then, the mobility of these complexes under electrophoretic conditions will only depend on their hydrodynamic sizes in a sieving matrix, and smaller proteins will have higher mobility. However, SDS-PAGE is a labor-intensive and time-consuming method and the many different manual operations are sources of irreproducibility. This is the reason why capillary gel electrophoresis (CGE) has known a significant interest from the scientific community since the 90s and is now also recognized as an important analytical tool in the biopharmaceutical industry for the characterization of mAbs. Indeed, CGE is the adaptation of the traditional slab gel electrophoresis into the capillary format, by using soluble polymers to create a replaceable molecular sieve for separating molecules based on size differences. In addition, it is also possible to automate the sample preparation, to further reduce the analyst "hand-on" time and total assay time.[155] CGE offers a variety of advantages including ease of handling, automated operation, better resolving power, and increased throughput. Today, there are several companies that offer commercial sieving kits to run CGE. Various recent works have confirmed the clear benefits of CGE over SDS-PAGE, with obvious improvements in terms of precision and resolution. As an example, Shi et al.[156] have evaluated the precision of migration time and quantitative performance for the analysis of light chain and heavy chain of mAbs. In their study, RSD values were less than 0.5% for migration time and less than 5% for corrected peak area in CGE, using electrokinetic injection (usual injection mode for CGE). By switching to hydrodynamic injection and using internal standards, Cianciulli et al.[157] could improve the precision of the CGE assay with RSDs on migration time and peak area of 0.2% and 1−2%, respectively. However, since the sensitivity was reduced with hydrodynamic injection, the sample concentration and injection volume were adjusted to achieve sufficient S/N ratio (>70). This result suggests that the method can be considered for stability testing methods and CGE can replace SDS-PAGE for mAb purity determination. To further improve the performance of CGE, microchip CGE devices were developed. Because of the short capillary length and high separation efficiency, microchip CGE is a high-throughput method, able to separate size variants in a few seconds to a few minutes. Obviously, the performance of microchip-based CGE has been compared to that of CGE. Similar resolving power has been demonstrated when analyzing the degradation species of thermally stressed mAbs under regular CGE and microchip CGE. In that particular study performed with commercial instrumentation, the analysis time was reduced by a factor of 20.[158] As an alternative to microchip CGE, multicapillary gel electrophoresis (mCGE) systems with covalent fluorescent labeling were developed, allowing highly sensitive and fast analysis of mAbs (purity assessment and subunit characterization).[159]

CGE-LIF of APTS labeled N-glycans is widely and routinely applied in biopharmaceutical industries to determine the N-glycan profiles.[160−162] APTS introduces three negative charges and a fluorophoric group in the glycans allowing highly efficient, fast, and sensitive separations. Hamm et al. recently described the identification of all of the major and most of the minor glycans in a mAb produced in NS0 cells. Since CGE is not MS compatible, structures were identified through the use of standards or a battery of exoglycosidases, among others.[163] A multisite N-glycan mapping study was recently performed to evaluate the reproducibility of sample preparation and analysis of N-glycans using CGE of APTS-labeled glycans with LIF detection. Low variability and high reproducibility, both within any given site as well across all sites, were demonstrated, indicating that a standard N-glycan analysis platform appropriate for general use (clone selection, process development, lot release, etc.) within the industry can be established.[160] Reusch et al. compared CGE with LIF detection to the gold standard N-glycan analysis method based on HILIC and 2-AB labeling. Next to APTS-labeled glycans, 8-aminonaphthalene-1,3,6-trisulfonate (ANTS) labeled N-glycans were analyzed. Consistent results in terms of precision and accuracy were obtained.[47] The same groups described the development of an automated high-throughput N-glycan analysis method with multiplexing CGE-LIF on a DNA analyzer.[164] Peak assignment was conducted by HILIC separation and MS/MS identification of the APTS-labeled glycans combined with peak fractionation and subsequent CGE-LIF analysis of the characterized fractions. This method, also referred to as DNA-sequencer-aided fluorophore-assisted carbohydrate electrophoresis (DSA-FACE), allows 96 samples to be analyzed in parallel and the overall platform offers a throughput of 3 000 samples/day.[47,164] To assist the identification of CGE glycan peaks, tools have recently been developed to automatically calculate the glucose unit (GU) values for all sample components of interest in an electropherogram with a concomitant database search for structural assignment.[165,166]

DOI: 10.1021/acs.analchem.5b04561
Anal. Chem. 2016, 88, 480−507

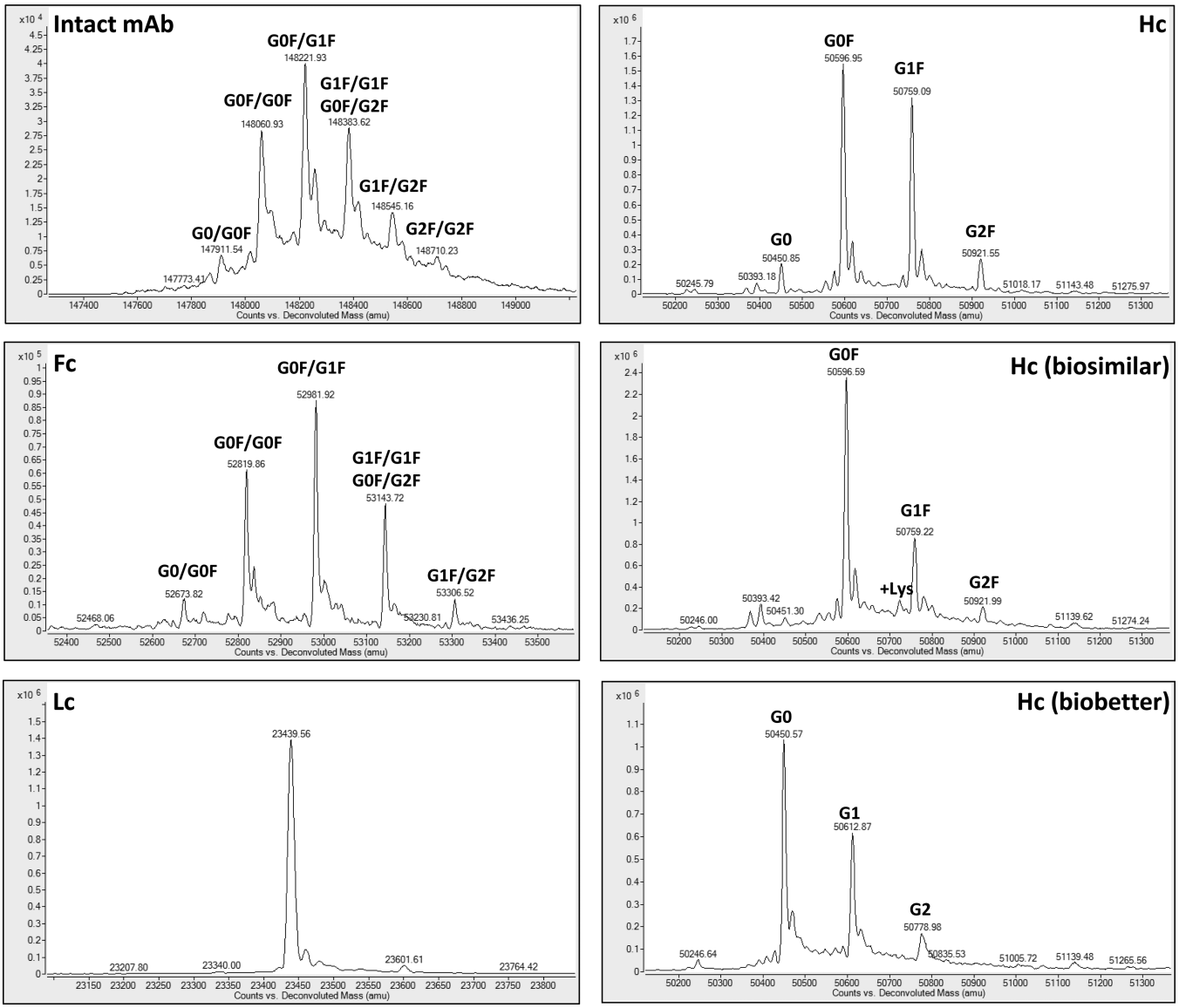


Figure 8. Deconvoluted spectra of trastuzumab (Herceptin), its biosimilar and biobetter acquired using Q-TOF-MS. Shown are the intact mAb, Fc (generated following papain digestion), Lc and Hc (generated following DTT reduction). Reprinted from *J. Chromatogr. A*, Vol. *1335*, Sandra, K.; Vandenheede, I.; Sandra, P., Modern chromatographic and mass spectrometric techniques for protein biopharmaceutical characterization, pp 81–103 (ref 16). Copyright 2014, with permission from Elsevier.

MASS SPECTROMETRIC APPROACHES

Mass spectrometry is an indispensable tool in the characterization of protein biopharmaceuticals. It is unthinkable to submit dossiers to the authorities without having intensive MS characterization data incorporated in it. From MS data, one can retrieve accurate molecular weight and amino acid sequence information, the N- and C-termini, co- and post-translational modifications and modification sites, DAR, drug load distribution and conjugation sites, sequence variants, higher order structures, etc.[16,20,24] These measurements demand for high-resolution accurate mass instruments with MS/MS capabilities. Historically, quadrupole time-of-flight (Q-TOF) systems have dominated the biopharmaceutical landscape but in recent years they have been challenged by hybrid Orbitrap MS systems. When surveying the literature it can be concluded that the majority of MS measurements of biopharmaceuticals make use of ESI to present the molecules as gas-phase ions to the mass spectrometer. While ESI is commonly performed under denaturing conditions using organic solvents and acids, recent years has witnessed an increased interest in native ESI using volatile buffers at neutral pH. MALDI has also been used but suffers from poor mass accuracy and resolution for larger molecules. This is a direct result of the limited charging of molecules using the latter ionization mode (predominantly $[M + H]^+$), requiring the use of TOF mass analyzers in low-resolution linear mode, to capture the m/z values generated from proteins. As pointed out before, characterizing protein biopharmaceuticals requires a measurement at different levels and one often refers to intact protein, middle-up, top-down, middle-down, and bottom-up measurements in the specialized MS literature.[20]

With clear benefits being demonstrated in protein analysis over the years, ion mobility (IM) has also been adopted in biopharmaceutical analysis. The latter separates gas-phase ions according to their size and shape in a drift cell at the millisecond time scale prior to m/z measurement and gives

DOI: 10.1021/acs.analchem.5b04561
Anal. Chem. 2016, 88, 480–507

higher order structural information. To perform MS/MS experiments on proteins, peptides, and glycans, a wide range of fragmentation modes are available. Collision-induced dissociation (CID) is most commonly used but extra features are offered by alternative fragmentation modes such as electron transfer dissociation (ETD), electron capture dissociation (ECD), etc. In biopharmaceutical analysis, the MS systems are typically and preferably combined with one of the earlier described chromatographic and electrophoretic techniques. This can be done in an offline or online manner. While RPLC and HILIC are directly compatible with MS, the MS measurement of peaks from HIC, IEX, and SEC, i.e., chromatographic modes making use of nonvolatile salts, typically requires their desalting.[16] As discussed earlier, this issue can be tackled when using 2D-LC in a heart-cutting setup.[46,70] In recent years, the combination of CZE to MS has also become more attractive with the commercial introduction of sheathless interfaces providing enhanced sensitivity over sheath-flow interfaces. The different MS strategies will be reviewed in the following paragraphs.

Intact Protein and Middle-Up Measurements. Intact protein and middle-up measurements refer to the determination of the MW of proteins or of large fragments thereof (Fc, Fab, Fc/2, $F(ab')_2$, Fd, Hc, Lc) and associated heterogeneities which can nowadays be obtained with low mass errors (<0.005%). Sandra et al. reported on the Q-TOF measurement of intact trastuzumab as well as the Lc, Hc, and Fc fragments (Figure 8).[16] Such a measurement provides an initial confirmation of the gene-derived protein sequence, reveals structural integrity, as well as PTMs. In this example, the existence of several glycoforms with characteristic 146 and 162 Da spacings indicative for fucose and galactose, and consequently N-glycosylation, is demonstrated. The middle-up Hc data was compared to the data acquired from a biosimilar and glyco-engineered biobetter in development. In the former case, it was revealed that the glycosylation was qualitatively similar to the originator product yet differed from a quantitative perspective. In the latter case, it was demonstrated that glycans lack the core fucose, an essential feature to increase the ADCC. Reusch et al. compared middle-up measured glycosylation profiles to the gold standard method using 2-AB labeling of released N-glycans and HILIC separation.[111] The Hc, generated following reduction, or Fc/2, generated following IdeS cleavage, were infused in a Q-TOF-MS system. It was concluded that the Hc method is not suited for a detailed N-glycosylation characterization, since only the four major glycoforms were observed. However, it is very useful for the high-throughput analysis of the main glycan species. In the measurement of Fc/2, 12 glycan species could be detected of which 11 could be quantified. This is a direct result of the lower MW associated with the latter giving less peak overlap. Both the Hc and Fc/2 methods were shown to be precise and accurate. Biacchi et al. characterized the N-glycosylation of cetuximab by middle-up offline CZE−UV combined with MALDI and ESI-MS measurements using a TOF analyzer.[123] Cetuximab is a particular mAb that contains, next to the glycosylation site in the Fc region, an additional site in the variable region of the Hc. MWs were measured for six charge variants detected in the CZE separation of IdeS treated cetuximab. It was demonstrated that ESI results in the read-out of the various glycoforms in the Fc/2 and $F(ab')_2$ fragments. MALDI, on the other hand, gave rise to a single broad peak for all these measurements. Regarding the Fc/2 domain, two C-terminal lysine variants were identified and separated and the glycosylation on the variants was revealed. Eight glycoforms were detected in the $F(ab')_2$ domain and separated in three different CZE peaks based on the presence of N-glycolylneuraminic acid. By performing intact and middle-up measurements on cetuximab, Ayoub et al. revealed a sequence error in the reported sequence of the Lc in databases and publications and achieved a comprehensive characterization of the glycosylation on both the Fab and Fc domains.[38] A total of 24 glycans were measured and quantified on the Fc/2 and Fd fragments. The authors clearly pointed out that these are critical experiments that biosimilar developers need to conduct. Henninot et al. directly measured glycosylation profiles from cell culture supernatant using LC−TOF-MS.[167] By combining IdeS and EndoS digestion, the latter removing the distal glycan heterogeneity, fucosylation yield could easily be determined on Fc/2. Spahr et al. recently characterized the O-glycosylation of glycine−serine linkers in recombinant Fc-fusion proteins measured using TOF-MS following their reduction.[168] Glycoforms were successfully measured before and after the removal of the Fc N-glycans using PNGase F. A heterogeneous population of O-glycans with a xylose core decorated with galactose, glucuronic acid, N-acetylglucosamine, N-acetylneuraminic acid, as well as phosphate was observed.

Intact protein and middle-up measurements also revealed a Lc extension of a recombinant IgG1 produced in a CHO cell line which could be explained by a single base-pair mutation in a stop codon resulting in translation until the next stop codon. The extension of 17 amino acids was observed upon analyzing the intact IgG1 and could be linked to the Lc upon analyzing a reduced sample using TOF-MS. The Lc extension was approximately 13.6% of wild type Lc. The sequence was subsequently confirmed by peptide mapping, N-terminal Edman degradation of collected peaks, and DNA sequencing.[169] Scott et al. also identified a C-terminal extension in 2 candidate CHO clones which could be explained by a DNA rearrangement.[170] Initially observed as new peaks in CEX and CGE, intact protein and middle-up TOF-MS analysis showed larger than expected masses on a subpopulation. Bottom-up MS/MS measurements combined with *de novo* sequencing and database searching against the DNA vector revealed that the extension was derived from the Lc vector nontranslated sequence which was inserted prior to the C-terminal lysine of the Hc sequence. The authors stressed that their findings demonstrate the value of mass spectrometry testing even at early phases of development. Evidently, these clones were not taken further in development and more promising clones were selected. Using ESI-TOF-MS, Lu et al. identified a collected SEC peak, located between the mAb monomer and dimer in the SEC profile. The peak contained the mAb with one and two extra light chains. The C-terminal cysteine of the extra Lc was either a free thiol, capped by glutathione, cysteine, or another light chain.[54]

Bispecific mAbs are composed of two different half antibody (Lc + Hc) arms, each of which recognizes a distinct antigen and therefore have attracted substantial therapeutic interest. The proper association of the individual Lc and Hc has shown to be challenging. MS has been used to reveal the heterodimeric purity of bispecific mAbs following their deglycosylation by detecting and quantifying homodimeric (~150 kDa) and half antibody (~75 kDa) impurities.[171] The assay was capable of detecting impurities at levels as low as 0.6% and simultaneously allowed an assessment of C-terminal lysine truncation. Macchi

DOI: 10.1021/acs.analchem.5b04561
Anal. Chem. 2016, 88, 480−507

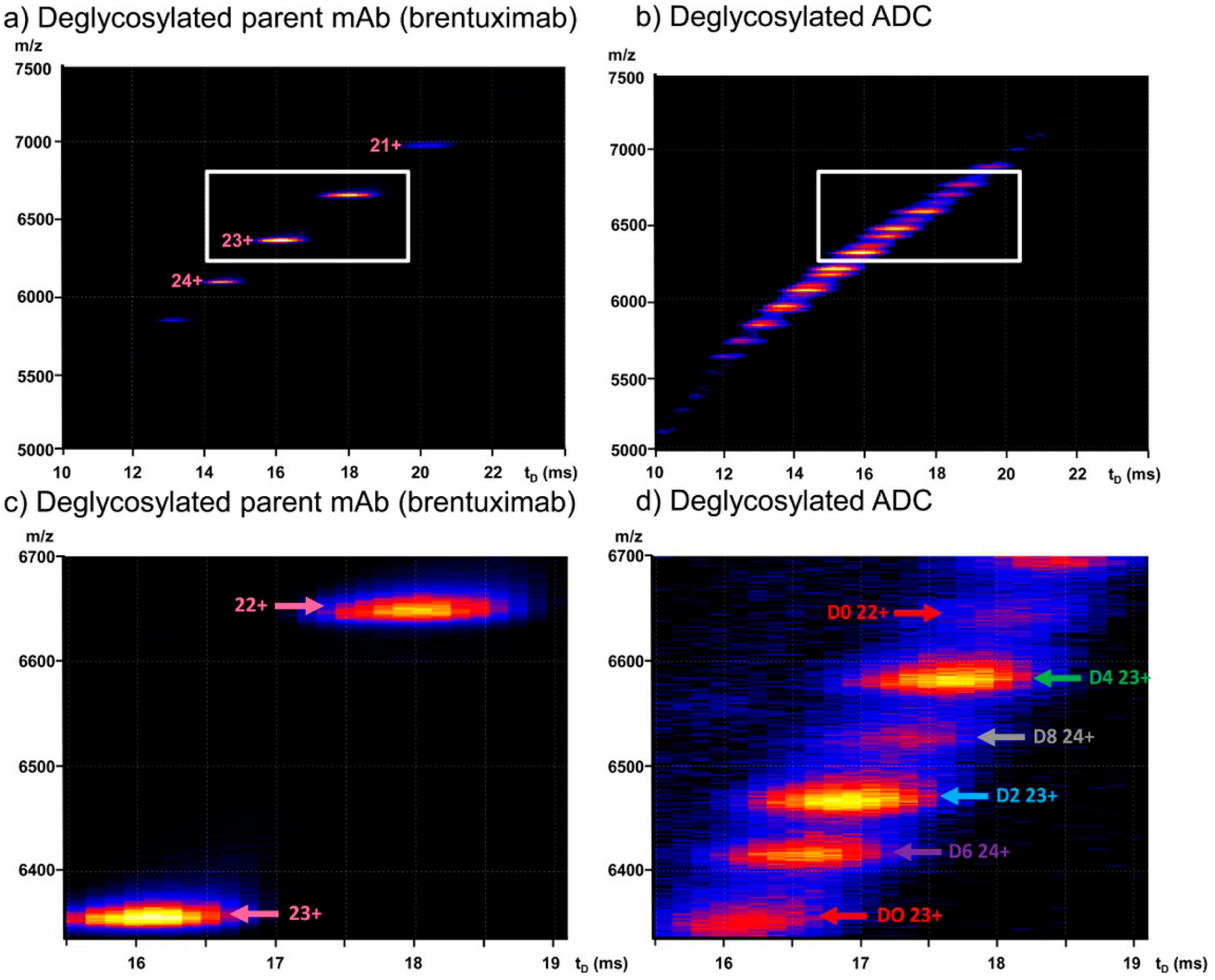


Figure 9. Native IM-MS analysis of unconjugated brentuximab and brentuximab vedotin. Reproduced from Debaene, F.; Boeuf, A.; Rousset, E.W.; Colas, O.; Ayoub, D.; Corvaia, N.; Dorsselaer, A.V.; Beck, A.; Cianférani, S. *Anal. Chem.* **2014**, *86*, 10674−10683 (ref 68). Copyright 2014 American Chemical Society.

et al. described the absolute quantitation of product related variants of bispecific mAbs and focused on the measurement of half antibodies as a surrogate for noncovalent homodimers.[172] These half antibodies result from the nondenaturing conditions used in the RPLC−TOF-MS method. Using standard addition, homodimers could be quantified at levels as low as 0.2%.

Next to measuring the relative large mass shifts described above, the intact protein and middle-up measurements furthermore allow one to assess minor mass deviations that results from events like deamidation (+1 Da), oxidation (+16 Da), cyclization (−17 or −18 Da), etc. This typically necessitates the combination with an upfront chromatographic or electrophoretic separation. The detection of a Lc deamidation (+1 Da) and partial (+2 Da) and full reduction (+4 Da) of intrachain disulfide bridges was recently highlighted by combining a RPLC separation with Q-TOF-MS.[16] In the absence of this chromatographic step, these modifications would be hidden under the nonmodified Lc peak. Forstenlehner et al. recently described an LC−MS approach for characterizing oxidation on the intact PEGylated recombinant human granulocyte-colony stimulating factor (rhG-CSF, pegfilgrastim).[92] This represents a challenge due to the overlapping protein charge state pattern and polyethylene glycol (PEG) polydispersity. To minimize spectral overlap, charge reduction by means of the addition of triethylamine was applied. Singly, doubly and triply oxidized species were readily resolved in the chromatogram, while their oxidation status was easily determined from the mass shifts observed in the mass spectra.

ADCs have successfully been subjected to mass spectrometric measurement.[22,23,173] In cases where the conjugation process takes place on reduced cysteine residues, the mAb structure is maintained through noncovalent interactions demanding for special care to transfer them to the gas-phase. Valliere-Douglas et al. were the first to report the successful intact mass measurement of ADCs conjugated at interchain cysteine residues. A volatile buffer at neutral pH was used to present deglycosylated ADCs under native conditions to the Q-TOF-MS.[57] The removal of the N-glycans facilitated spectral interpretation. A very similar approach was undertaken by Chen et al. to determine the DAR of ADCs.[174] After removal of the cytotoxic drug using a cysteine protease, thereby leaving the linker intact, consistent DAR read-outs were reported compared to HIC, the gold standard method for DAR

DOI: 10.1021/acs.analchem.5b04561
Anal. Chem. 2016, 88, 480−507

determination. It was indeed demonstrated that the presence of the hydrophobic drugs affected ionization efficiency. Under native conditions, the charged envelop of a protein shifts to higher m/z values (>m/z 4 000), which are readily measurable with TOF instruments. The earlier generation Orbitrap systems, however, did not allow native measurements given their limited m/z range. Rosati et al. described the measurement of ADCs using native MS on a modified Orbitrap.[175] The system offered sufficient resolution to simultaneously measure glycosylation induced heterogeneity in parallel with the drug load in a single analysis. Debaene et al. took the DAR and drug distribution assessment of interchain cysteine linked ADCs one step further by incorporating ion mobility in the workflow (Figure 9).[68] The potential of native IM-MS was compared to native MS and HIC, using glycosylated and deglycosylated brentuximab vedotin, the sole commercial cysteine linked ADC, and fractions collected from the latter method were also analyzed. All drug loaded species were separated by native IM-MS and similar DAR values were obtained compared to native MS and HIC. The same study also compared Q-TOF data with higher resolution Orbitrap data. Both systems performed equally well in the determination of the DAR, but the latter was shown to be more advantageous to measure glycosylated mAbs. The same group acquired denaturing and native MS spectra on a glycosylated and deglycosylated lysine conjugated ADC, i.e., trastuzumab emtansine, using Q-TOF and Orbitrap MS systems.[176] The authors concluded that it is advisible to determine the DAR on raw spectra instead of deconvoluted spectra and that spectra obtained by native MS are much simpler than those obtained under denaturing conditions. Native IM-MS data were also acquired and used to determine the average DAR and drug load profile. Huang et al. further elaborated upon the utility of IM-MS for DAR measurements.[177] They demonstrate that analyte cleanup in the gas-phase provides significant improvements of signal-to-noise allowing accurate DAR measurements. While the above-described studies report the measurement of intact ADCs, middle-up analyses of cysteine conjugated ADCs have as well been described. The LC−MS analysis of IdeS treated and reduced ADCs allowed the determination of the drug loading and distribution of Lc and Fd fragments as well as the average DAR. Analysis of the Fc/2 fragment in the same run furthermore provided insights in glycosylation.[91] By measuring the Lc and Hc of reduced IgG1 and IgG2 ADCs, it could be revealed that IgG1 mAbs favor conjugation to the cysteines between the Lc and Hc, whereas IgG2s demonstrate preference for the hinge region cysteines.[178]

Native MS evidently has applications beyond the characterization of ADCs.[179,180] Rosati et al. reported on the detailed qualitative and quantitative glycosylation analysis of IgG4 half antibody mutants (~75 kDa). More than 20 different complex N-glycans could be assigned and over 30 proteoforms resulting from the combination of glycosylation and C-terminal glycine truncation could be revealed in a single spectrum.[175] Thompson et al. analyzed complex mixtures of antibodies by native Orbitrap MS.[181] Mixtures of mAbs aim to mimic the native immune response of polyclonal serum and are promising therapeutics. Up to 15 deglycosylated antibodies with MW around 150 kDa could be simultaneously analyzed at high mass accuracy (average 7 ppm) in the absence of a chromatographic step. Baseline resolution was achieved between antibodies differing in MW by 50 Da, while it was still possible to differentiate two mAbs differing by 21 Da. The authors state that the ability to resolve these two species is near the achievable physical limit as the isotopic envelope for a mAb is 25 Da at full with at half-maximum (fwhm). Woodard et al. simultaneously analyzed mixtures of antibodies to determine the aggregation propensity during candidate selection.[56] Monomers were separated from aggregates using nondenaturing SEC and the individual mAbs in the mixture were identified by TOF-MS and quantified relative to an unstressed control. Eight intact mAbs and $F(ab')_2$ fragments could simultaneously be analyzed and distinguished in the deconvoluted TOF-MS spectra. Native MS has furthermore been used to probe global conformational changes/differences and to study the interaction between protein biopharmaceuticals and their targets.[24,180] A recent study revealed that oxidation of a specific heavy chain methionine resulted in a stepwise reduction of mAb/human neonatal Fc receptor complex formation. This complex is important since it dictates antibody half-life.[182] When combining native MS with IM, great structural details can be obtained. Native IM-MS has been used to monitor the dynamics of IgG4 Fab arm exchange and bispecific mAb formation.[183] The method furthermore allowed characterizing the mAb/antigen complex formation. Conformational differences resulting from different S−S bonding networks in IgG2 have as well been revealed by native IM-MS.[184]

Top-Down and Middle-Down Measurements. While the above-described intact protein and middle-up studies are highly valuable, they have in recent years been complemented with gas-phase fragmentation to obtain additional information regarding the structure, sequence, modifications, and modification sites. This procedure is typically called top-down or middle-down depending whether intact proteins or large fragments are being fragmented. Gas-phase fragmentation of proteins mainly relies on ECD and ETD and to a lesser extent on CID. Top-down studies on intact antibodies using Fourier transform ion cyclotron (FTICR) MS with ECD fragmentation and Orbitrap with ETD fragmentation were recently described and resulted in sequence coverages of around 35%, thereby outperforming ETD and CID on Q-TOF and CID on Orbitrap.[185,186] Mao et al. demonstrated the potential of top-down MS but clearly stated that two major challenges remain preventing its widespread use: (1) generation of more sequence coverage throughout the entire molecule and (2) reliable site-specific localization of PTMs and potential sequence variants.[186] It was quickly recognized that the existence of S−S bridges limits the sequence coverage and, in solving this critical issue, Zhang et al. described the electrochemistry assisted top-down characterization of disulfide containing proteins.[187] Sequence coverage in both CID and ECD based top-down analysis was significantly improved after electrochemical reduction of the disulfide bonds. Nicolardi et al. were the first to apply this strategy on mAbs.[188] Further providing an answer to the limited sequence coverage obtained in top-down analysis of mAbs, Fornelli et al. described the middle-down analysis of IdeS treated and reduced mAbs.[189] The 25 kDa Fc/2, Lc, and Fd fragments were analyzed by RPLC coupled with an ETD enabled Orbitrap system. Sequence coverage reached 50% in a single run and 70% when merging data from independent runs. In addition, methionine oxidation sites could be identified and a proof-of-concept toward the measurement of antibody mixtures was demonstrated. The authors state that, compared to bottom-up measurements, the approach limits the introduction of sample preparation artifacts such as deamidation given the short IdeS digestion time. Wang et al. took this

DOI: 10.1021/acs.analchem.5b04561
Anal. Chem. 2016, 88, 480−507

approach one step further and performed intact protein, middle-up, and middle-down measurement on collected CEX peaks of an anti-*Clostridium difficile* IgG1 mAb.[190] Middle-down measurements were performed on the Lc and Hc using higher-energy collisional dissociation (HCD) and fragments were measured in an Orbitrap MS. Clipping sites in the heavy and light chains and oxidation of three heavy chain methionine residues were demonstrated. Pang et al. reported very recently on the use of pepsin-containing membranes for the online generation of middle-down fragments from mAbs and reported high sequence coverage for the Lc after performing CID, ETD, and HCD fragmentation using an Orbitrap MS system.[191] In addition, oxidation and deamidation sites could be revealed on the Lc and Hc. Forstenlehner et al. performed the site-specific characterization and absolute quantification of pegfilgrastim oxidation using top-down LC−MS, thereby further building on their intact protein LC−MS method which could not make a distinction between the different oxidation sites.[93] Site-specific quantification was obtained through all-ion fragmentation in the HCD cell of an Orbitrap MS. Several diagnostic y-ions were generated allowing the assessment of the oxidation state of the four methionine residues. Dyachenko et al. reported native MS/MS measurements on the interchain cysteine conjugated ADC brentuximab vedotin using a modified Orbitrap for high m/z measurements equipped with a high mass quadrupole selector.[192] MS/MS experiments allowed to localize the drug molecules in the ADC and as such to calculate the percentage of each positional isomer in the sample. The authors found a fair agreement with the data reported by Le et al., who combined HIC and CGE to profile the positional isomers on a similar ADC.[66] Top-down MS has as well been used to study higher order structures.[24] Tian et al. performed collision induced unfolding of native antibodies in the gas-phase, prior to IM-MS analysis which allowed the rapid characterization of disulfide bonding patterns, glycosylation, and higher order structure.[193] It has been hypothesized that top-down fragmentation combined with native ESI preferably occurs in flexible regions providing more site-specific information for conformational changes revealed by IM-MS.[24,184] The higher order structural characterization of intact therapeutic antibodies using hydrogen−deuterium exchange (HDX), subzero temperature chromatography, and ETD on an Orbitrap MS system was recently described.[194,195] Domain level deuteration information was obtained for 6 IgG domains on Herceptin, and ligand binding induced structural differences were determined to be located only on the variable region of the Lc. The authors point out that the presence of disulfide bonds prevents the method from being able to obtain amino acid level structural information within the disulfide linked regions. Nevertheless, the simplicity associated with the method prevents back-exchange, and the throughput makes it well suited for assessing higher order structural comparability between antibodies, e.g., biosimilar and originator.

MALDI, making use of in-source decay (ISD), has as well successfully been used for top- and middle-down sequencing.[196] Ayoub et al. used MALDI for the middle-down characterization of cetuximab after the collection of Fc/2, Fd, and Lc separated by RPLC.[38] Combining top- and middle-down analyses with multiple fragmentation techniques including ETD, ECD, and MALDI-ISD, Tran et al. characterized a reference mAb and a fusion IgG protein in great detail. Sequence coverages of 35.9% and 52.6% for mAb Hc and Lc and 61% for the fusion protein were obtained.[197]

Bottom-Up Measurements. The enormous amount of information that can be obtained using the above-described MS-based approaches do, however, not show the complete picture. While intact protein and middle-up measurements give insight in identity and modifications, they do not provide the amino acid sequence nor do they allow the localization of modifications. In theory, this gap should be filled by top-down and middle-down MS experiments. Being still at its infancy, the latter can currently not compete with bottom-up MS in terms of sequence coverage and determination of modifications as well as modification sites. Bottom-up measurements refer to the MS and MS/MS analysis of peptides generated from the protein following enzymatic digestion using high quality proteases like trypsin, chymotrypsin, AspN, GluC, and LysC. While the majority of bottom-up measurements make use of trypsin, a promising alternative has recently been described.[198] The secreted aspartic protease 9 (Sap9) from *C. albicans* generates larger fragments (3.5 kDa on average) from mAbs and gives rise to less sample preparation artifacts (e.g., deamidation) as a result of the lower digestion pH. The bottom-up approach relies on the combination of RPLC or CZE with MS. Since these separation techniques typically do not resolve all peptides in protein digests, the additional separation based on m/z in high-resolution Q-TOF or Orbitrap MS systems significantly increases sequence coverage and allows highlighting low levels of PTMs. In the majority of applications, MS/MS is used to sequence the peptides, thereby increasing the confidence of the identifications and to further locate modifications. CID is commonly employed, since it fragments in a predictable manner along the peptide bond with the generation of y- and b-ions containing the C- and N-terminus of the peptides, respectively. The mass difference between successive y- and b-ions corresponds to the residual mass of the amino acids. As such, spectra arise that can easily be interrogated by software algorithms allowing automated data analysis. All MS vendors nowadays have powerful biopharmaceutical supporting software in their portfolio. While CID maintains stable modifications like oxidation and deamidation on the peptide backbone, labile modifications such as glycosylation and phosphorylation are preferentially cleaved making it challenging to determine their sites of modification. Other fragmentation techniques like ETD or ECD further assist in these cases.[16]

Full MS sequence coverage with simultaneous identification of abundant and low abundant modifications like glycosylation, deamidation, aspartate isomerization, oxidation, pyroglutamate formation, and lysine truncation from a single sheathless CZE−Q-TOF-MS analysis of mAb tryptic digests has been demonstrated.[132−134] Using CID, respectively, 70 and 90% of the y- and b-ions were covered for cetuximab and trastuzumab.[132] Full sequence coverage on trastuzumab originator and biosimilars, together with disulfide bridges, deamidation, oxidation, C-terminal lysine truncation, etc., was also reported by Chen et al. using multienzyme digestions and LC−MS/MS with CID and ETD on an Orbitrap system.[199] The authors also performed a nontargeted omics type strategy, globally comparing ion intensities between samples, and as such revealed a double mutation in one of the biosimilars. Bottom-up LC−MS measurements further supported the functional characterization of chemical modification sites in the complementary-determining regions (CDRs) of a recombinant IgG1.[200] Forced degradation was applied to the mAb, modification sites and levels were determined by LC−MS

DOI: 10.1021/acs.analchem.5b04561
Anal. Chem. 2016, 88, 480−507

based peptide mapping and functional evaluation was achieved by surface plasmon resonance (SPR) analysis. Several methionine (oxidation) and asparagine (deamidation) residues as well as a lysine residue (glycation) were identified as potential critical quality attributes (CQAs). Wang et al. developed a LC−MS based peptide mapping method to quantify mAb deamidation at a detection limit of 0.1%.[201] The method was qualified as a characterization test for comparability studies, forced degradation studies, and characterizing reference standards. In another work, the use of a chymotryptic peptide mapping method was described to identify and characterize a deamidated form of an IgG1 which was observed as an acidic peak in CEX. The deamidation, located in the Fc region was missed by tryptic peptide mapping because the peptides were hydrophilic and eluted near the void volume.[202] An elegant LC−MS method was recently developed for the accurate determination of methionine oxidation using stable isotope labeling.[203] Methionine sulfoxide is a potential CQA that is challenging to determine accurately as it is a common sample preparation and analysis artifact that is easily overestimated. Oxidizing the study sample with hydrogen peroxide enriched with ^{18}O atoms prior to sample preparation results in full conversion of methionine to methionine sulfoxide preventing further downstream oxidation. The ratio of $^{16}O/^{18}O$ methionine sulfoxide was used to calculate the true level of oxidation. Much lower levels of oxidation were demonstrated when using this method compared to classical LC−MS based peptide mapping. ^{18}O labeling has as well been used for assigning aspartyl/isoaspartyl products from asparagine deamidation and aspartic acid isomerization.[204]

Reusch et al. compared glycosylation profiles obtained at the glycopeptide level to the method using HILIC separation of 2-AB labeled glycans.[111] Glycopeptide measurements furthermore varied in the mass analyzer, i.e., Q-TOF or Orbitrap, ionization technique, i.e., ESI or MALDI, and sample introduction, i.e., direct infusion or RPLC. At first instance, quantitative analysis of glycans using MS seems contradictory. Indeed, the analysis of sialic acid, phosphate and sulfate containing glycans is challenging given the ionization differences compared to neutral glycans. In addition, in-source fragmentation, especially involving sialic acid containing glycans, further hampers quantitative measurements. Indeed, slightly lower values of G0F and higher values of G0F minus *N*-acetylglucosamine were reported compared to the reference HILIC method. Despite that, the glycopeptide method identifies and quantifies an equal number of glycans in a precise manner. Shah et al. compared mAb glycan profiles obtained at glycopeptide level to those obtained at glycan level using HPAEC, RPLC, and HILIC and concluded that the former method is a viable alternative.[205] Li et al. took this glycopeptide measurement into practice and compared the glycan profiles of commercial rituximab (Mabthera) and an anti-CD20 mAb developed using RNA interference (RNAi) to decrease core fucosylation and, hence, improve ADCC.[206] This biobetter indeed demonstrated <30% core fucose compared to >90% for rituximab originator. Two mutations, however, were detected in the biobetter but PTMs including disulfide bridges, free cysteines, N-terminal pyroglutamate formation, C-terminal lysine truncation, methionine oxidation, and asparagine deamidation were very similar between both products. A recent study reported on the influence of glycosylation on trypsin digestion by performing a relative quantification of glycopeptides derived from the conserved Fc glycosylation site.[207] A clear bias in digestion was observed depending on the type of glycosylation but this was largely dependent on the intact higher order structure and was substantially reduced when performing digestions in denaturing conditions.

Next to N-glycosylation, various protein biopharmaceuticals also carry O-glycans on their serine and/or threonine residues. Analyzing O-glycosylation, however, is challenging from several perspectives. With harsh chemical liberation being the only viable option to "universally" release O-glycans, glycan heterogeneity is very often assessed at glycopeptide level. As discussed earlier, Spahr et al. studied O-glycosylation on glycine-serine linkers in recombinant Fc-fusion proteins.[168] While abundant O-glycans could be revealed by middle-up measurement following PNGase F treatment, much more insight was obtained when performing analysis at the glycopeptide level. Glycosylation was indeed shown to be located on the $(G4S)_n$ linker region and mono, di, tri, tetra, and pentasaccharides all containing a xylose core further modified with galactose, glucuronic acid, *N*-acetylglucosamine, *N*-acetylneuraminic acid, as well as phosphate were observed. Structural information on the glycans was obtained from accurate mass measurement combined with MS/MS, sialidase, and phosphatase treatment. Since CID was used, the actual sites of xylosylation could not be revealed. As mentioned earlier, CID typically does not maintain labile modifications onto the peptide backbone and in spectra of glycosylated peptides, the sugar fragments often dominate the peptide fragments because the glycosidic bonds are more labile than the peptide bonds.[16] The alternative fragmentation modes of ECD and ETD typically maintain labile modifications on the peptide backbone. In the absence of clear consensus sequences for O-glycosylation, bottom-up MS/MS measurement incorporating ETD or ECD are indispensable for assigning glycosylation sites.[75,208,209] Using the latter approach, Wen et al. assigned the O-xylosylation sites in proteins containing $(G4S)_n$ linkers and furthermore revealed that reduction of the level of xylosylation can be achieved by extensive clone selection and its elimination can be accomplished by site-directed mutagenesis.[209] These routes are worth exploring since O-glycans have the potential to be immunogenic. O-Glycosylation analysis of etanercept has as well been facilitated by bottom-up MS and MS/MS measurements. Twelve O-glycosylation sites, occupied with core 1 type O-glycans, were detected using ETD.[75]

Besides the more common PTMs, many other modifications have been revealed by bottom-up measurements. In a series of papers, Chumsae et al. described how bottom-up MS assisted in discovering antibody modifications, giving rise to acidic variants in CEX, originating from chemicals in the cell culture media or formulation buffer.[210−212] Citric acid, commonly used in formulation buffers in a pH range 3−6 and generally regarded as inert, was shown to covalently modify a mAb.[211] Peptide mapping revealed that the modification occurred at the N-terminus of the light chain. The authors concluded that one has to consider formulations as a potential source for chemical modifications and product heterogeneity. Methylglyoxal, a highly reactive metabolite that can be generated from glucose or lipids in culture medium, modified arginine residues in mAbs.[210] Xylosone, an oxidative product of ascorbic acid, a common additive to cell culture media to limit oxidative stress, also gave rise to mAb modifications.[212] Xylosone's carbonyl groups react with amines (N-termini and lysines) forming hemiaminal or Schiff base. The authors, who title their paper: "When Good Intentions Go Awry", stress that similar

DOI: 10.1021/acs.analchem.5b04561
Anal. Chem. 2016, 88, 480−507

modifications and mechanisms will likely be revealed in other systems and proteins. Using bottom-up measurements that combined absorption spectroscopy and MS, it was revealed that a color change of a light irradiated and heat-stressed mAb formulation originated from tryptophan-derived chromophores, i.e., oxidation products.[213] An elegant approach for the characterization of oxidative carbonylation on mAbs has recently been described.[214] The method involved the tagging of the highly reactive carbonyl groups with Girard's Reagent T followed by peptide mapping on high-resolution MS. The applicability of this approach was demonstrated by the identification of 14 common carbonylation sites on three similar IgG1s.

As mentioned earlier, using SEC, Lu et al. highlighted an extra peak between a mAb monomer and dimer.[54] Using intact protein measurements it was demonstrated that the mAb carried one and two extra light chains. Performing nonreducing and reducing LysC bottom-up measurements, it could be revealed that the extra light chains were linked to the mAb light chain through disulfide bonds. In general, confirmation of the correct disulfide linkage and demonstration of the lack of scrambled disulfide bonds are important to ensure the appropriate folding and structure of proteins. Currently, these analyses are typically achieved by performing multiple experiments, most commonly via the comparison of the samples with- and without reduction by LC−MS and MS/MS. To eliminate the need of multiple experiments and complicated data analysis, a simple LC−MS-based method coupled with postcolumn partial reduction was developed.[215] This method allows the simultaneous detection of the disulfide linked peptides and their corresponding free cysteine containing peptides in the same spectrum. Using a recombinant monoclonal IgG1 antibody, this method demonstrated the ability to confirm the correct disulfide linkage and the ability to detect scrambled disulfide bonds from a single experiment. As an alternative strategy, an electrochemical cell could be used for partial postcolumn reduction. Until now, this has not been described in the literature. Ni et al. used multienzyme digestions (LysC, trypsin, AspN, pepsin, and PNGase F) and LC−MS analysis using CID and ETD to assign the status of all 15 cysteine residues in recombinant human arylsulfatase.[216] Six disulfide bridges, two free cysteines, and one cysteine converted to formylglycine (for 70%) could be determined. Zhang et al. performed a detailed characterization of cysteine related variants, including hinge disulfide structural isomers, in an IgG2 antibody by performing bottom-up measurements.[217] Five RPLC fractions were generated and digested under nonreducing conditions. Free cysteine residues were labeled upfront with *N*-ethyl maleimide (NEM). In their comparison of the glycosylation profiles of commercial rituximab and a glyco-engineered biobetter, Li et al. demonstrated high similarity in disulfide bridges and free cysteine residues.[206] Disulfides were only correctly linked in case where digestions were performed at low pH using pepsin. In case where trypsin digestion was applied at pH 6.8, traces of scrambling were found. Scrambling increased significantly when digestion was performed at pH 8. Disulfide containing peptides were identified based on accurate mass measurement complemented with CID and ETD experiments. Both fragmentation modes are complementary and the latter allows the fragmentation of the disulfide bond.

LC−MS is furthermore indispensable in the characterization of sequence variants. Typically, these variants are picked up by intact protein or middle-up analysis and their origin is revealed by bottom-up MS measurements very often supported by DNA sequencing.[169,170,218,219] Ayoub et al. revealed a sequence error in the reported sequence of cetuximab in databases and publications by combining intact, middle-up, middle-down, and bottom-up MS experiments. Intact and middle-up measurements revealed a + 58 Da mass shift which was identified as an alanine/glutamic acid substitution at position 213 in the Lc following GluC based bottom-up LC−MS experiments.[38] The rationale for the use of GluC was that trypsin generated a small peptide in the region of interest. Nowadays, sequence variant analysis is often performed in an unbiased, proteomics-like manner in which bottom-up MS/MS data is analyzed by software programs which take all permutations in the sequence into account. A substantial number of false positives are, however, generated. Brady et al. recently reported on a procedure for the rapid assessment of sequence variants by mixing of two samples of an antibody with the same amino acid sequence in a dilution series followed by bottom-up measurements.[220] With this strategy, true hits were discriminated from false positives at levels as low as 0.1% using a simple linear regression analysis. They employed the method to measure sequence variants after a change in production scale (pilot to final scale) and to compare sequence variants in three biosimilars produced by different cell lines. To characterize N-terminal heterogeneities which might arise from truncation, fragmentation, and incomplete processing of the signal peptide, an in-gel derivatization of primary amines using (*N*-succinimidyloxycarbonylmethyl)-tris(2,4,6-trimethoxyphenyl)-phosphonium bromide (TMPP) followed by trypsin digestion and LC−MS/MS analysis was reported.[221] Unexpected sequence variants could be revealed at trace levels in mAbs and mAb mixtures.

Peptide mapping is particularly powerful to determine drug conjugation sites in ADCs. Janin-Bussat et al. showed the characterization of the drug loaded peptides of interchain cysteine conjugated brentuximab vedotin by LysC based peptide mapping.[222] To keep the hydrophobic drug loaded peptides in solution, digestion was performed in the presence of 10% acetonitrile, and 40% isopropanol was added postdigestion. The data confirmed that the drug was linked to the interchain cysteine residues. It was furthermore demonstrated that the drug was preferentially linked to the Cys220 when only one drug was bound to the Hc. When two drugs were bound to the Hc, they were preferentially linked to Cys 226 and Cys 229. Compared to conjugation at interchain cysteine residues (8 sites), conjugation at lysine residues (40 sites) gives rise to a substantially higher heterogeneity. Gautier et al. revealed mAb lysine residues susceptible to drug conjugation by bottom-up LC−MS using *N*-hydroxysuccinimide (NHS) based tandem mass tags.[223] Both very reactive (hot spots) and highly resistant lysine residues could be identified. Lysine residues in the vicinity of the glycan chain were shown to be less reactive.

The review clearly illustrates that the characterization of biopharmaceuticals requires a wide range of technologies and methodologies as well as a multilevel (protein, peptide, glycan) approach. This is perhaps best illustrated in the papers of Visser et al. and Jung et al. detailing the comparability assessment of, respectively, rituximab and infliximab biosimilars to the originator products.[34,72] Dozens of techniques, including the chromatographic, electrophoretic, and mass spectrometric techniques described in this review, were involved, this to comprehensively characterize all attributes of the mAbs. To simplify this process, a quantitative bottom-up mass spectrom-

DOI: 10.1021/acs.analchem.5b04561
Anal. Chem. 2016, 88, 480−507

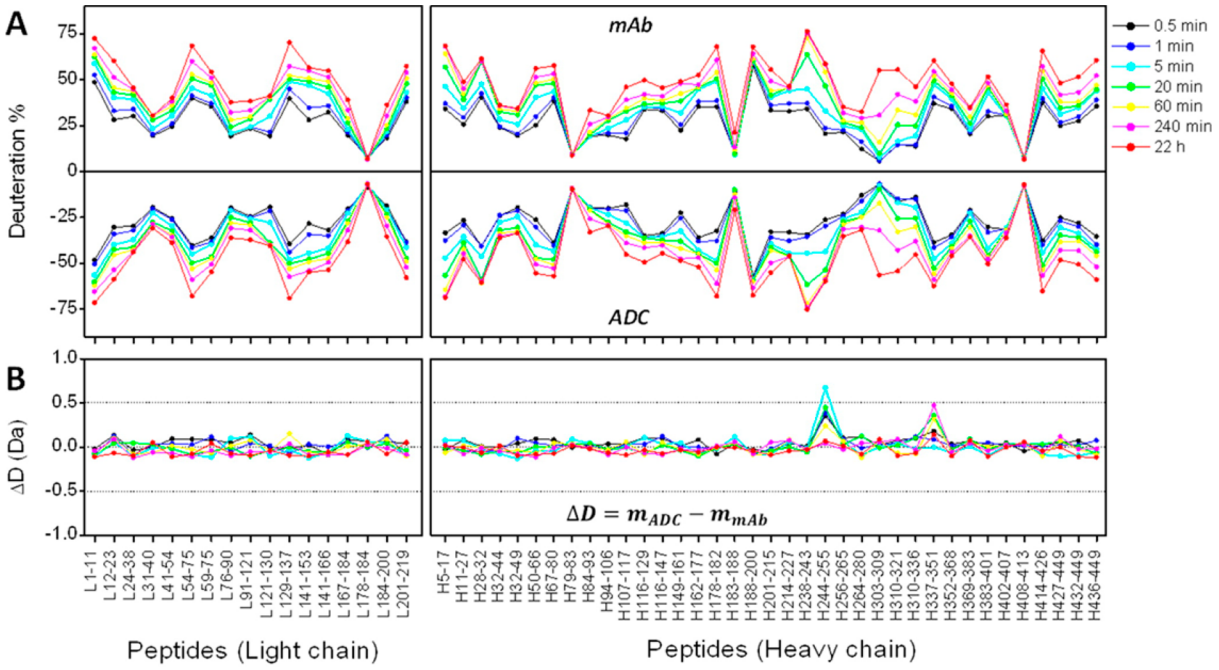


Figure 10. Comparison of HDX plots obtained on naked mAb and cysteine linked ADC. The upper figures (A) plot the deuterium uptake in function of peptide for both the mAb and ADC. Colored lines represent the deuterium labeling time. The lower figure (B) plots the mass difference of individual peptides from the mAb and ADC at each labeling time. Two regions (H244−H255 and H337−H351) in the ADC are shown to be more structurally dynamic and/or solvent exposed. These minor local conformational changes are due to the partial loss of interchain disulfide bonds. Reproduced from Pan, L.Y.; Salas-Solano, O.; Valliere-Douglass, J.F. *Anal. Chem.* **2014**, *86*, 2657−2664 (ref 229). Copyright 2014 American Chemical Society.

etry multiattribute method has recently been described for the characterization and quality control testing of biopharmaceuticals in one single analysis and in fully automated mode.[224] The trypsin based peptide mapping method uses a combination of high-mass accuracy/high-resolution MS data generated by Orbitrap MS and automated identification and relative quantification of PTMs with dedicated software. The authors stress that the method has the potential to replace several conventional electrophoretic and chromatographic methods currently used in QC to release products. The output was compared to the traditional assays to assess deamidation (CEX), glycosylation (HILIC), and clipping (CGE) and very good correlations were demonstrated. Several groups are exploring the use of MS in QC which clearly makes sense in view of the multiattribute monitoring bottom-up MS method described by Rogers et al.[224] To prevent the generation, and subsequent reporting, of low quality data, Zhou et al. described a strategy to evaluate the performance metrics of bottom-up LC−MS workflows based on Q-TOF and Orbitrap platforms.[225] A bovine serum albumin (BSA) digest, spiked with synthetic peptides present at 0.1% to 100% of the BSA digest peptide concentration, was used. A workflow for system suitability testing is described.

It is clear that bottom-up LC−MS measurements are extensively used to determine the amino acid sequence and analyze PTMs and has become an integral part of the regulatory approval process. One might not immediately see the link between bottom-up MS and higher order structural analysis since all structural information is lost upon generating peptides. Higher order structures can nevertheless be interrogated at peptide level. In its simplest form, limited proteolysis can provide insight in higher order structure but one nowadays relies on more advanced tools such as cross-linking, footprinting, and hydrogen−deuterium exchange (HDX), among others.[24,226]

HDX is especially promising and is quickly being implemented in biopharmaceutical analysis but requires a substantial user expertise.[226] Upon placing a protein in a D_2O solution, amide hydrogens can exchange with deuterium based on their solvent accessibility. Exposed and dynamic regions exchange rapidly, while rigid and protected regions exchange more slowly. Bottom-up measurements following labeling allow the discrimination of these regions (due to the mass shift induced by deuterium) and as such provide an indirect read-out of the higher order structure. To prevent back-exchange, digestions are performed at low pH typically using pepsin and separations are performed at low temperatures. Dedicated HDX systems are available on the market. In recent years, HDX has been used to determine the conformations of the different charge variants of a mAb.[227] The charge variants could be attributed to C-terminal lysine deamidation, sialylation, and oxidation. Four CEX fractions were collected and subjected to HDX bottom-up measurements. Results demonstrated that charge variants were not different in terms of conformation and solution dynamics. Using HDX, Zhang et al. demonstrated conformational differences between the three major human IgG2 hinge disulfide isoforms and linked it to functional aspects, i.e., antigen binding.[228] Pan et al. compared interchain cysteine linked IgG1 ADC and the corresponding mAb by HDX.[229] Approximately 100 peptic peptides were identified accounting for sequence coverage of 95%, allowing a comprehensive HDX experiment. It was demonstrated that ADC and mAb share very similar conformation and dynamics (~90%). Two Fc regions in the former were shown to be more structurally dynamic and/or solvent accessible, which was due to the absence of intact interchain disulfide bonds and not to

DOI: 10.1021/acs.analchem.5b04561
Anal. Chem. 2016, 88, 480−507

the presence of the cytotoxic drug (Figure 10). In a subsequent work, the same authors demonstrated that the site-specific drug conjugation at an engineered Cys residue at the position 239 of Hc does not impact the structural integrity of antibodies and thereby demonstrate the relevance of HDX experiments in understanding the individual contributions of site-mutagenesis and drug-linker conjugation on the higher order structure of therapeutic candidate ADCs.[230] The technique has furthermore been used in recent years to assess comparability between originator mAb and biosimilar,[34] to study how mAb structural changes are connected with aggregation,[231] to study antigen−antibody binding (epitope mapping),[232] etc. HDX experiments performed on mAbs require the rapid reduction of the disulfide bonds under acidic and cold conditions demanding for high TCEP concentrations. Electrochemical reduction as a substitute for TCEP reduction has recently been reported, and trastuzumab sequence coverages of 96% and 87% for, respectively, Hc and Lc were demonstrated.[233,234] While HDX is reversible, and as such prone to back exchange, irreversible labeling has as well been described to assess higher order characteristics. Labeling can be site-specific (e.g., carboxyl group labeling using glycine ethyl ester)[235] or nonspecific (e.g., hydroxyl radical labeling).[24,184,236] These so-called footprinting techniques have been used to locate mAb dimer interaction sites,[236] to reveal conformational differences resulting from different S−S bonding networks in IgG2[184] and to map epitopes,[237] among others.

Glycan MS Measurements. Both ESI and MALDI-MS are widely used for profiling and structural characterization of labeled and unlabeled glycans.[238] Reusch et al. benchmarked MALDI-TOF-MS against other glycan analysis methods including HILIC of 2-AB labeled glycans and concluded that, apart for the sialic acid containing glycans, results are very comparable to those of the latter reference method.[111] In addition, data can be acquired in a high-throughput manner. Loss of sialic acids, a common phenomenon in MALDI, can be avoided by permethylation or carboxyl group derivatization.[239] This simultaneously allows to distinguish between α2,3 and α2,6 linked sialic acids. When implementing glycan stabilization, Reusch et al. observed low levels of sialylated glycans not detected in the absence of the derivatization step.[111] Using ^{13}C-enriched glycans as internal standards, Echeverria et al. turned the profiling of glycans by MALDI-TOF into a rapid and robust method for glycan identification and absolute quantification.[240]

ESI-MS of glycans is either applied in infusion mode or with an up-front separation (HILIC, CZE). Wang et al. reported on deviating core fucose quantity when comparing CGE-LIF of APTS labeled N-glycans to direct infusion ESI-MS of underivatized N-glycans and attributed this to in-source fragmentation.[241] Indeed, care is needed upon interpreting glycan MS data and implementing a separation step clearly simplifies data interpretation. As discussed earlier, recent years witnessed the introduction of various tags to enhance ESI efficiency.[81,82] The presence of a label at the reducing terminus is clearly beneficial in reading the MS/MS data. Glycans undergo two types of cleavage upon CID, glycosidic cleavages between two monosaccharides providing information on composition and sequence and cross-ring cleavages that involve fragmentation of the sugar ring providing detail on the linkage type. MS/MS experiments performed on glycans reveal hexose, *N*-acetylhexosamine, deoxyhexose based on mass values. The identity of the monosaccharides, i.e., mannose, galactose, *N*-acetylglucosamine, and fucose, is typically inferred by making assumptions based on the compound class and biosynthetic rules.[16]

CONCLUDING REMARKS

The structural characterization of protein biopharmaceuticals heavily relies on state-of-the-art chromatography, electrophoresis, and mass spectrometry. Using an array of methodologies applied at protein, peptide, glycan, and amino acid levels, a detailed insight in primary structure, in post-translational modifications, in higher order structures, etc. can be assessed. These methods are extensively being applied during the development of the drug, and a subset of validated methods is subsequently used to monitor the critical quality attributes in a routine environment, prior to clinical and commercial release. Next to the determination of the above-described product-related characteristics, chromatography, electrophoresis, and mass spectrometry are also appearing at the forefront in the measurement of process-related impurities, i.e., host-cell proteins (HCP),[242,243] and in bioanalysis, i.e., to determine pharmacokinetic properties (PK)[244] or the *in vitro* and *in vivo* fate of ADCs.[245,246] These characteristics have historically been determined using ligand binding assays, but MS based approaches are nowadays becoming widely accepted.

AUTHOR INFORMATION

Corresponding Author

*E-mail: koen.sandra@richrom.com.

Notes

The authors declare no competing financial interest.

Biographies

Szabolcs Fekete holds a Ph.D. degree in analytical chemistry from the Technical University of Budapest, Hungary. He worked at the Chemical Works of Gedeon Richter Plc at the analytical R and D department for 10 years. Since 2011, he is working at the University of Geneva in Switzerland. He contributed 70+ journal articles and authored book chapters in handbooks. His main interests include liquid chromatography, column technology, and pharmaceutical and protein analysis.

Davy Guillarme holds a Ph.D. degree in analytical chemistry from the University of Lyon, France. He is now senior lecturer at the University of Geneva in Switzerland. He authored 140 journal articles related to pharmaceutical analysis. His expertise includes HPLC, UHPLC, HILIC, LC−MS, SFC, analysis of proteins, and mAbs. He is an editorial advisory board member of several journals including *Journal of Chromatography A*, *Journal of Separation Science*, *LC−GC North America*, and others.

Pat Sandra is emeritus from the Ghent University, Belgium and Founder-Director of the Research Institute for Chromatography, Kortrijk, Belgium. He is author of more than 500 peer-reviewed publications and has been active in all fields of separation science and mass spectrometry. His present interest is focused on high-resolution techniques for the characterization of small and macro pharmaceuticals and on automation in sample preparation.

Koen Sandra received a Ph.D. degree in biochemistry from the Ghent University, Belgium, in 2005. After his Ph.D., he joined Pronota, a molecular diagnostics company located in Ghent, Belgium. In 2008, he joined the Research Institute for Chromatography, Kortrijk, Belgium, where he currently holds the position of Scientific Director. His research focuses on the chromatographic, electrophoretic and mass spectrometric analysis of (bio)pharmaceuticals, proteins, metabolites,

DOI: 10.1021/acs.analchem.5b04561
Anal. Chem. 2016, 88, 480−507

lipids, etc. As a nonacademic scientist, he is author of over 40 highly cited scientific papers.

■ ACKNOWLEDGMENTS

Davy Guillarme wishes to thank the Swiss National Science Foundation for support through a fellowship to Szabolcs Fekete (Grant 31003A_159494). Pat and Koen Sandra furthermore acknowledge many colleagues from the biopharmaceutical industry for transferring some of their challenging analytical problems and the entire biopharma-team at the Research Institute for Chromatography for providing solutions.

■ REFERENCES

(1) Walsh, G. *Nat. Biotechnol.* **2014**, *32* (10), 992−1000.
(2) Aggarwal, R. *Nat. Biotechnol.* **2014**, *32* (1), 32−39.
(3) Elvin, J. G.; Couston, R. G.; van der Walle, C. F. *Int. J. Pharm.* **2013**, *440* (1), 83−98.
(4) Ecker, D. M.; Jones, S. D.; Levine, H. L. *mAbs* **2015**, *7* (1), 9−14.
(5) Buss, N. A. P. S.; Henderson, S. J.; McFarlane, M.; Shenton, J. M.; de Haan, L. *Curr. Opin. Pharmacol.* **2012**, *12* (5), 615−622.
(6) Perez, H. L.; Cardarelli, P. M.; Deshpande, S.; Gangwar, S.; Schroeder, G. M.; Vite, G. D.; Borzilleri, R. M. *Drug Discovery Today* **2014**, *19* (7), 869−881.
(7) Panowski, S.; Bhakta, S.; Raab, H.; Polakis, P.; Junutula, J. R. *mAbs.* **2014**, *6* (1), 34−45.
(8) Chari, R. V. J.; Miller, M. L.; Widdison, W. C. *Angew. Chem., Int. Ed.* **2014**, *53* (15), 3796−3827.
(9) Weiner, L. M.; Surana, R.; Wang, S. *Nat. Rev. Immunol.* **2010**, *10* (5), 317−327.
(10) Beck, A.; Reichert, J. M. *mAbs* **2014**, *6* (1), 15−17.
(11) Sassoon, I.; Blanc, V. *Methods Mol. Biol.* **2013**, *1045*, 1−27.
(12) Berkowitz, S. A.; Engen, J. R.; Mazzeo, J. R.; Jones, G. B. *Nat. Rev. Drug Discovery* **2012**, *11*, 527−540.
(13) Epstein, M. S.; Ehrenpreis, E. D.; Kulkarni, P. M. *Am. J. Gastroenterol.* **2014**, *109*, 1856−1859.
(14) Beck, A.; Sanglier-Cianferani, S.; Van Dorsselaer, A. *Anal. Chem.* **2012**, *84* (11), 4637−4646.
(15) Sandra, K.; Vandenheede, I.; Dumont, E.; Sandra, P. *LC-GC Eur.* **2015**, *10* (Suppl), 16−23.
(16) Sandra, K.; Vandenheede, I.; Sandra, P. *J. Chromatogr. A* **2014**, *1335*, 81−103.
(17) Beck, A.; Reichert, J. M. *mAbs* **2013**, *5* (5), 621−623.
(18) Colwell, J. *Cancer Discovery* **2015**, *5* (5), 460.
(19) Fekete, S.; Gassner, A. L.; Rudaz, S.; Schappler, J.; Guillarme, D. *TrAC, Trends Anal. Chem.* **2013**, *42*, 74−83.
(20) Beck, A.; Wagner-Rousset, E.; Ayoub, D.; Van Dorsselaer, A.; Sanglier-Cianferani, S. *Anal. Chem.* **2013**, *85* (2), 715−736.
(21) Liu, H.; Ponniah, G.; Zhang, H. M.; Nowak, C.; Neill, A.; Gonzalez-Lopez, N.; Patel, R.; Cheng, G.; Kita, A. Z.; Andrien, B. *mAbs* **2014**, *6* (5), 1145−1154.
(22) Wakankar, A.; Chen, Y.; Gokarn, Y.; Jacobson, F. S. *mAbs* **2011**, *3* (2), 161−172.
(23) Alley, S. C.; Anderson, K. E. *Curr. Opin. Chem. Biol.* **2013**, *17* (3), 406−411.
(24) Zhang, H.; Cui, W.; Gross, M. L. *FEBS Lett.* **2014**, *588* (2), 308−317.
(25) Fekete, S.; Veuthey, J. L.; Guillarme, D. *J. Chromatogr. A* **2015**, *1408*, 1−14.
(26) Fekete, S.; Guillarme, D. *TrAC, Trends Anal. Chem.* **2014**, *63*, 76−84.
(27) Fekete, S.; Beck, A.; Guillarme, D. *Am. Pharm. Rev.* **2015**, *18*, 59−63.
(28) Fekete, S.; Beck, A.; Fekete, J.; Guillarme, D. *J. Pharm. Biomed. Anal.* **2015**, *102*, 33−44.
(29) Fekete, S.; Beck, A.; Fekete, J.; Guillarme, D. *J. Pharm. Biomed. Anal.* **2015**, *102*, 282−289.
(30) Rea, J. C.; Freistadt, B. S.; McDonald, D.; Farnan, D. *J. Chromatogr. A* **2015**, *1424*, 77−85.
(31) Fekete, S.; Beck, A.; Veuthey, J. L.; Guillarme, D. *J. Pharm. Biomed. Anal.* **2015**, *113*, 43−55.
(32) Abzalimov, R. R.; Frimpong, A.; Kaltashov, I. A. *Int. J. Mass Spectrom.* **2012**, *312*, 135−143.
(33) Szekeres, Z. K.; Olajos, M.; Ganzler, K. *J. Pharm. Biomed. Anal.* **2012**, *69*, 185−195.
(34) Visser, J.; Feuerstein, I.; Stangler, T.; Schmiederer, T.; Fritsch, C.; Schiestl, M. *BioDrugs* **2013**, *27* (5), 495−507.
(35) Pace, A. L.; Wong, R. L.; Zhang, Y. T.; Kao, Y. H.; Wang, Y. J. *J. Pharm. Sci.* **2013**, *102* (6), 1712−1723.
(36) Labrijn, A. F.; Meesters, J. I.; Priem, P.; De Jong, R. N.; Van den Bremer, E. T.; Van Kampen, M. D.; Gerritsen, A. F.; Schuurman, J.; Parren, P. W. *Nat. Protoc.* **2014**, *9*, 2450−2463.
(37) Beck, A.; Reichert, J. M. *mAbs* **2011**, *3*, 415−416.
(38) Ayoub, D.; Jabs, W.; Resemann, A.; Evers, W.; Evans, C.; Main, L.; Baessmann, C.; Wagner-Rousset, E.; Suckau, D.; Beck, A. *mAbs* **2013**, *5*, 699−710.
(39) Chen, X.; Nguyen, M.; Jacobson, F.; Ouyang, J. *mAbs* **2009**, *1*, 563−571.
(40) Joshi, V.; Kumar, V.; Rathore, A. S. *J. Chromatogr. A* **2015**, *1406*, 175−185.
(41) Zhang, L.; Patapoff, T.; Farnan, D.; Zhang, B. *J. Chromatogr A* **2013**, *1272*, 56−64.
(42) Talebi, M.; Shellie, R. A.; Hilder, E. F.; Lacher, N. A.; Haddad, P. R. *Anal. Chem.* **2014**, *86* (19), 9794−9799.
(43) Talebi, M.; Nordborg, A.; Gaspar, A.; Lacher, N. A.; Wang, Q.; He, X. Z.; Haddad, P. R.; Hilder, E. F. *J. Chromatogr. A* **2013**, *1317*, 148−154.
(44) Kang, X.; Kutzko, J. P.; Hayes, M. L.; Frey, D. D. *J. Chromatogr. A* **2013**, *1283*, 89−97.
(45) Rea, J. C.; Moreno, T.; Lou, Y.; Farnan, D. *J. Pharm. Biomed. Anal.* **2011**, *54*, 317−323.
(46) Stoll, D. R.; Harmes, D. C.; Danforth, J.; Wagner, E.; Guillarme, D.; Fekete, S.; Beck, A. *Anal. Chem.* **2015**, *87*, 8307−8315.
(47) Reusch, D.; Haberger, M.; Maier, B.; Maier, M.; Kloseck, R.; Zimmermann, B.; Hook, M.; Szabo, Z.; Tep, S.; Wegstein, J.; Alt, N.; Bulau, P.; Wuhrer, M. *mAbs* **2015**, *7*, 167−179.
(48) Cook, M. C.; Kaldas, S. J.; Muradia, G.; Rosu-Myles, M.; Kunkel, J. P. *J. Chromatogr. B: Anal. Technol. Biomed. Life Sci.* **2015**, *997*, 162−178.
(49) Fekete, S.; Beck, A.; Veuthey, J. L.; Guillarme, D. *J. Pharm. Biomed. Anal.* **2014**, *101*, 161−173.
(50) Barth, H. G.; Saunders, G. D. *LC-GC N. Am.* **2012**, *7*, 544−563.
(51) Fekete, S.; Ganzler, K.; Guillarme, D. *J. Pharm. Biomed. Anal.* **2013**, *78−79*, 141−149.
(52) Yang, R.; Tang, Y.; Zhang, B.; Lu, X.; Liu, A.; Zhang, Y. T. *J. Pharm. Biomed. Anal.* **2015**, *109*, 52−61.
(53) Farnan, D.; Moreno, G.; Stults, J.; Becker, A.; Tremintin, G.; Van Gils, M. *J. Chromatogr. A* **2009**, *1216*, 8904−8909.
(54) Lu, C.; Liu, D.; Liu, H.; Motchnik, P. *mAbs* **2013**, *5* (1), 102−113.
(55) Liu, H.; Bulseco, G.; Chumsae, C. *J. Am. Soc. Mass Spectrom.* **2009**, *20*, 2258−2264.
(56) Woodard, J.; Lau, H.; Latypov, R. F. *Anal. Chem.* **2013**, *85*, 6429−6436.
(57) Valliere-Douglas, J. F.; McFee, W. A.; Salas-Solano, O. *Anal. Chem.* **2012**, *84*, 2843−2849.
(58) Rea, J. C.; Lou, Y.; Cuzzi, J.; Hu, Y.; Jong, I.; Wang, Y. J.; Farnan, D. *J. Chromatogr. A* **2012**, *1270*, 111−117.
(59) Rea, J. C.; Moreno, G. T.; Vampola, L.; Lou, Y.; Haan, B.; Tremintin, G.; Simmons, L.; Nava, A.; Wang, Y. J.; Farnan, D. *J. Chromatogr. A* **2012**, *1219*, 140−146.
(60) Cockrell, G. M.; Wolfe, M. S.; Wolfe, J. L.; Schöneich, C. *Mol. Pharmaceutics* **2015**, *12* (6), 1784−1797.
(61) Li, Y.; Gu, C.; Gruenhagen, J.; Zhang, K.; Yehl, P.; Chetwyn, N. P.; Medley, C. D. *J. Chromatogr. A* **2015**, *1393*, 81−88.

DOI: 10.1021/acs.analchem.5b04561
Anal. Chem. 2016, 88, 480−507

(62) Rustandi, R. R. Hydrophobic interaction chromatography to analyze glycoproteins. In *Glycosylation Engineering of Biopharmaceuticals: Methods and Protocols*; Beck, A., Ed.; Springer Science + Business Media: New York, 2013.
(63) Fekete, S.; Veuthey, J. L.; Guillarme, D. *LC−GC Eur.* **2015**, *10* (Suppl.), 8−15.
(64) Wiggins, B.; Shin, L. L.; Yamaguchi, H.; Ratnaswamy, G. *J. Pharm. Sci.* **2015**, *104*, 1362−1372.
(65) Haverick, M.; Mengisen, S.; Shameem, M.; Ambrogelly, A. *mAbs* **2014**, *6*, 852−858.
(66) Le, L. N.; Moore, J. M. R.; Ouyang, J.; Chen, X.; Nguyen, M. D. H.; Galush, W. J. *Anal. Chem.* **2012**, *84*, 7479−7486.
(67) Ouyang, J. *Methods Mol. Biol.* **2013**, *1045*, 275−283.
(68) Debaene, F.; Boeuf, A.; Wagner-Rousset, E. W.; Colas, O.; Ayoub, D.; Corvaia, N.; Van Dorsselaer, A.; Beck, A.; Cianférani, S. *Anal. Chem.* **2014**, *86*, 10674−10683.
(69) Ouellette, D.; Chumsae, C.; Clabbers, A.; Radziejewski, C.; Correia, I. *mAbs* **2013**, *5* (3), 432−444.
(70) Birdsall, R.; Shion, H.; Kotch, F. W.; Xu, A.; Porter, T. J.; Chen, W. *mAbs* **2015**, *7* (6), 1036−1044.
(71) Shang, T. Q.; Saati, A.; Toler, K. N.; Mo, J.; Li, H.; Matlosz, T.; Lin, X.; Schenk, J.; Ng, C. K.; Duffy, T.; Porter, T. J.; Rouse, J. C. *J. Pharm. Sci.* **2014**, *103* (7), 1967−1978.
(72) Jung, S. K.; Lee, K. H.; Jeon, J. W.; Lee, J. W.; Kwon, B. O.; Kim, Y. J.; Bae, J. S.; Kim, D. I.; Lee, S. Y.; Chang, S. J. *mAbs* **2014**, *6* (5), 1163−1177.
(73) Chevreux, G.; Faid, V.; Scohyers, J. M.; Bihoreau, N. *Glycobiology* **2013**, *23* (12), 1531−1546.
(74) An, Y.; Zhang, Y.; Mueller, H. M.; Shameem, M.; Chen, X. *mAbs* **2014**, *6* (4), 879−893.
(75) Houel, S.; Hilliard, M.; Yu, Y. Q.; McLoughlin, N.; Martin, S. M.; Rudd, P. M.; Williams, J. P.; Chen, W. *Anal. Chem.* **2014**, *86* (1), 576−584.
(76) Ponniah, G.; Nowak, C.; Gonzalez, N.; Miano, D.; Liu, H. *Anal. Chem.* **2015**, *87*, 2718−2726.
(77) Turyan, I.; Hronowski, X.; Sosic, Z.; Lyubarskaya. *Anal. Biochem.* **2014**, *446*, 28−36.
(78) Doherty, M.; Bones, J.; McLoughlin, N.; Telford, J. E.; Harmon, B.; DeFelippis, M. R.; Rudd, P. M. *Anal. Biochem.* **2013**, *442* (1), 10−18.
(79) Stöckmann, H.; Adamczyk, B.; Hayes, J.; Rudd, P. M. *Anal. Chem.* **2013**, *85* (18), 8841−8849.
(80) Cook, K. S.; Bullock, K.; Sullivan, T. *Biologicals* **2012**, *40* (2), 109−117.
(81) Lauber, M. A.; Yu, Y. Q.; Brousmiche, D. W.; Hua, Z.; Koza, S. M.; Magnelli, P.; Guthrie, E.; Taron, C. H.; Fountain, K. J. *Anal. Chem.* **2015**, *87*, 5401−5409.
(82) Kozak, R. P.; Tortosa, C. B.; Fernandes, D. L.; Spencer, D. I. *Anal. Biochem.* **2015**, *486*, 38−40.
(83) Gilar, M.; Yu, Y. Q.; Ahn, J.; Xie, H.; Han, H.; Ying, W.; Qian, X. *Anal. Biochem.* **2011**, *417* (1), 80−88.
(84) Periat, A.; Krull, I. S.; Guillarme, D. *J. Sep. Sci.* **2015**, *38*, 357−367.
(85) Vanhoenacker, G.; Vandenheede, I.; David, F.; Sandra, P.; Sandra, K. *Anal. Bioanal. Chem.* **2015**, *407*, 355−366.
(86) Fekete, S.; Rudaz, S.; Veuthey, J. L.; Guillarme, D. *J. Sep. Sci.* **2012**, *35*, 3113−3123.
(87) Fekete, S.; Beck, A.; Wagner, E.; Vuignier, K.; Guillarme, D. *J. Sep. Sci.* **2015**, *38*, 1−8.
(88) Vlasak, J.; Ionescu, R. *mAbs* **2011**, *3*, 253−263.
(89) Gritti, F.; Guiochon, G. *J. Chromatogr. A* **2011**, *1218*, 907−921.
(90) Fekete, S.; Veuthey, J. L.; Eeltink, S.; Guillarme, D. *Anal. Bioanal. Chem.* **2013**, *405*, 3137−3151.
(91) Wagner-Rousset, E.; Janin-Bussat, M. C.; Colas, O.; Excoffier, M.; Ayoub, D.; Haeuw, J. F.; Rilatt, I.; Perez, M.; Corvaïa, N.; Beck, A. *mAbs* **2014**, *6* (1), 173−184.
(92) Forstenlehner, I. C.; Holzmann, J.; Scheffler, K.; Wieder, W.; Toll, H.; Huber, C. G. *Anal. Chem.* **2014**, *86* (1), 826−834.
(93) Forstenlehner, I. C.; Holzmann, J.; Toll, H.; Huber, C. G. *Anal. Chem.* **2015**, *87* (18), 9336−9343.
(94) Fekete, S.; Guillarme, D. *LC-GC Eur.* **2012**, *25*, 540−550.
(95) Fekete, S.; Dong, M. W.; Zhang, T.; Guillarme, D. *J. Pharm. Biomed. Anal.* **2013**, *83*, 273−278.
(96) Fekete, S.; Berky, R.; Fekete, J.; Veuthey, J. L.; Guillarme, D. *J. Chromatogr. A* **2012**, *1236*, 177−188.
(97) Li, Y.; Rao, C.; Tao, L.; Wang, J.; Lorbetskie, B.; Girard, M. *J. Pharm. Biomed. Anal.* **2014**, *88*, 123−129.
(98) Schuster, S. A.; Wagner, B. M.; Boyes, B. E.; Kirkland, J. J. *J. Chromatogr. A* **2013**, *1315*, 118−126.
(99) Liu, H.; Jeong, J.; Kao, Y. H.; Zhang, Y. T. *J. Pharm. Biomed. Anal.* **2015**, *109*, 142−149.
(100) Fekete, S.; Jensen, D. S.; Zukowski, J.; Guillarme, D. *J. Chromatogr. A* **2015**, *1414*, 51−59.
(101) Bobály, B.; Guillarme, D.; Fekete, S. *J. Pharm. Biomed. Anal.* **2015**, *104*, 130−136.
(102) Hayes, R.; Myers, P.; Edge, T.; Zhang, H. *Analyst* **2014**, *139*, 5674−5677.
(103) Ahmed, A.; Ritchie, H.; Myers, P.; Zhang, H. *Adv. Mater.* **2012**, *24*, 6042−6048.
(104) Ahmed, A.; Abdelmagid, W.; Ritchie, H.; Myers, P.; Zhang, H. *J. Chromatogr. A* **2012**, *1270*, 194−203.
(105) Fekete, S.; Guillarme, D. *J. Chromatogr. A* **2013**, *1320*, 86−95.
(106) Bobály, B.; Guillarme, D.; Fekete, S. *J. Sep. Sci.* **2014**, *37*, 189−197.
(107) Berky, R.; Fekete, S.; Fekete, J. *Chromatographia* **2012**, *75*, 305−312.
(108) Lauber, M. A.; Koza, S. M.; McCall, S. A.; Alden, B. A.; Iraneta, P. C.; Fountain, K. J. *Anal. Chem.* **2013**, *85* (14), 6936−6944.
(109) Higel, F.; Demelbauer, U.; Seidl, A.; Friess, W.; Sörgel, F. *Anal. Bioanal. Chem.* **2013**, *405* (8), 2481−2493.
(110) Michael, C.; Rizzi, A. M. *J. Chromatogr. A* **2015**, *1383*, 88−95.
(111) Reusch, D.; Haberger, M.; Falck, D.; Peter, B.; Maier, B.; Gassner, J.; Hook, M.; Wagner, K.; Bonnington, L.; Bulau, P.; Wuhrer, M. *mAbs* **2015**, *7*, 732−742.
(112) Hanneman, A. J.; Strand, J.; Huang, C. T. *J. Pharm. Sci.* **2014**, *103* (2), 400−408.
(113) Song, T.; Ozcan, S.; Becker, A.; Lebrilla, C. B. *Anal. Chem.* **2014**, *86* (12), 5661−5666.
(114) Oh, M. J.; Hua, S.; Kim, B. J.; Jeong, H. N.; Jeong, S. H.; Grimm, R.; Yoo, J. S.; An, H. J. *Bioanalysis* **2013**, *5* (5), 545−559.
(115) Kenny, D. T.; Gaunitz, S.; Hayes, C. A.; Gustafsson, A.; Sjöblom, M.; Holgersson, J.; Karlsson, N. G. *Methods Mol. Biol.* **2013**, *988*, 145−167.
(116) Zhao, S. S.; Chen, D. D. Y. *Electrophoresis* **2014**, *35*, 96−108.
(117) He, Y.; Mo, J.; Xiaoping, H.; Ruesch, M. *Capillary Electrophoresis and Microchip Capillary Electrophoresis: Principles, Application and Limitations*, 1st ed.; Garcia, C. D., Chumbimuni-Torres, Y., Carrilho, E., Eds.; John Wiley: Hoboken, NJ, 2013; pp 293−308.
(118) Creamer, J. S.; Oborny, N. J.; Lunte, S. M. *Anal. Methods* **2014**, *6*, 5427−5449.
(119) Gassner, A. L.; Rudaz, S.; Schappler, J. *Electrophoresis* **2013**, *34*, 2718−2724.
(120) Batz, N. G.; Mellors, J. S.; Alarie, J. P.; Ramsey, J. M. *Anal. Chem.* **2014**, *86*, 3493−3500.
(121) Redman, E. A.; Batz, N. G.; Mellors, J. S.; Ramsey, J. M. *Anal. Chem.* **2015**, *87*, 2264−2272.
(122) Tamizi, E.; Jouyban, A. *Electrophoresis* **2015**, *36*, 831−858.
(123) Biacchi, M.; Gahoual, R.; Said, N.; Beck, A.; Leize-Wagner, E.; François, Y. N. *Anal. Chem.* **2015**, *87* (12), 6240−6250.
(124) Shi, Y.; Li, Z.; Qiao, Y.; Lin, J. *J. Chromatogr. B: Anal. Technol. Biomed. Life Sci.* **2012**, *906*, 63−68.
(125) Moritz, B.; Schnaible, V.; Kiessig, S.; Heyne, A.; Wild, M.; Finkler, C.; Christians, S.; Mueller, K.; Zhang, L.; Furuya, K.; Hassel, M.; Hamm, M.; Rustandi, R.; He, Y.; Salas-Solano, O.; Whitmore, C.; Ae Park, S.; Hansen, D.; Santos, M.; Lies, M. *J. Chromatogr. B: Anal. Technol. Biomed. Life Sci.* **2015**, *983*, 101−110.

DOI: 10.1021/acs.analchem.5b04561
Anal. Chem. 2016, 88, 480−507

(126) He, Y.; Isele, C.; Hou, W.; Ruesch, M. *J. Sep. Sci.* **2011**, *34*, 548−555.
(127) Espinosa-De la Garza, C.; Perdomo-Abundez, F. C.; Padilla-Calderon, J.; Uribe-Wiechers, J. M.; Perez, N. O.; Flores-Ortiz, L. F.; Medina-Rivero, E. *Electrophoresis* **2013**, *34*, 1133−1140.
(128) Wheeler, T. D.; Sun, J. L.; Pleiner, S.; Geier, H.; Dobberthien, P.; Studts, J.; Singh, R.; Fathollahi, B. *Anal. Chem.* **2014**, *86* (11), 5416−5424.
(129) Whitmore, C. D.; Gennaro, L. A. *Electrophoresis* **2012**, *33* (11), 1550−1556.
(130) Kašička, V. *Electrophoresis* **2015**, DOI: 10.1002/elps.201500329.
(131) Wenz, C.; Barbas, C.; Lopez-Gonzalvez, A.; Garcia, A.; Benavente, F.; Sanz-Nebot, V.; Blanc, T.; Freckleton, G.; Britz-McKibbin, P.; Shanmuganathan, M.; de l'Escaille, F.; Far, J.; Haselberg, R.; Huang, S.; Huhn, C.; Pattky, M.; Michels, D.; Mou, S.; Yang, F.; Neusuess, C.; Tromsdorf, N.; Baidoo, E. E. K.; Keasling, J. D.; Park, S. S. *J. Sep. Sci.* **2015**, *38*, 3262−3270.
(132) Gahoual, R.; Busnel, J. M.; Beck, A.; Francois, Y. N.; Leize-Wagner, E. *Anal. Chem.* **2014**, *86*, 9074−9081.
(133) Gahoual, R.; Burr, A.; Busnel, J. M.; Kuhn, L.; Hammann, P.; Beck, A.; Francois, Y. N.; Leize-Wagner, E. *mAbs* **2013**, *5*, 479.
(134) Lew, C.; Gallegos-Perez, J. L.; Fonslow, B.; Lies, M.; Guttman, A. *J. Chromatogr. Sci.* **2015**, *53* (3), 443−449.
(135) Gahoual, R.; Biacchi, M.; Chicher, J.; Kuhn, L.; Hammann, P.; Beck, A.; Leize-Wagner, E.; Francois, Y. N. *mAbs* **2014**, *6*, 1464−1473.
(136) Biacchi, M.; Bhajun, R.; Saïd, N.; Beck, A.; François, Y. N.; Leize-Wagner, E. *Electrophoresis* **2014**, *35* (20), 2986−2995.
(137) Mellors, J. S.; Black, W. A.; Chambers, A. G.; Starkey, J. A.; Lacher, N. A.; Ramsey, J. M. *Anal. Chem.* **2013**, *85*, 4100−4106.
(138) Bunz, S. C.; Cutillo, F.; Neusüß, C. *Anal. Bioanal. Chem.* **2013**, *405* (25), 8277−8284.
(139) Bunz, S. C.; Rapp, E.; Neusüß, C. *Anal. Chem.* **2013**, *85* (21), 10218−10224.
(140) Volpi, N.; Maccari, F. *Methods Mol. Biol.* **2013**, *984*, 27−43.
(141) Jooß, K.; Sommer, J.; Bunz, S. C.; Neusüß, C. *Electrophoresis* **2014**, *35* (9), 1236−1243.
(142) Jayo, R. G.; Thaysen-Andersen, M.; Lindenburg, P. W.; Haselberg, R.; Hankemeier, T.; Ramautar, R.; Chen, D. D. Y. *Anal. Chem.* **2014**, *86*, 6479−6486.
(143) Zhao, S. S.; Chen, D. D. Y. *Electrophoresis* **2014**, *35*, 96−108.
(144) Creamer, J. S.; Oborny, N. J.; Lunte, S. M. *Anal. Methods* **2014**, *6*, 5427−5449.
(145) Anderson, C. L.; Wang, Y.; Rustandi, R. R. *Electrophoresis* **2012**, *33* (11), 1538−1544.
(146) Cao, J.; Sun, W.; Gong, F.; Liu, W. *Electrophoresis* **2014**, *35* (10), 1461−1468.
(147) Salas-Solano, O.; Kennel, B.; Park, S. S.; Zhang, X.; Zhang, L.; Sosic, Z.; Boumajny, B.; Zeng, M.; Cheng, K. C.; Reed-Bogan, A.; Cummins-Bitz, S.; Michels, D. A.; Parker, M.; Bonasia, P.; Hong, M.; Cook, S.; Ruesch, M.; Lamb, D.; Bolyan, D.; Kiessig, S.; Allender, D.; Nunnally, B. *Chromatographia* **2011**, *73*, 1137−1144.
(148) Salas-Solano, O.; Kennel, B.; Park, S. S.; Roby, K.; Sosic, Z.; Boumajny, B.; Free, S.; Reed-Bogan, A.; Michales, D.; McElroy, W.; Bonasia, P.; Hong, M.; He, X.; Ruesch, M.; Moffatt, F.; Kiessig, S.; Nunnally, B. *J. Sep. Sci.* **2012**, *35*, 3124−3129.
(149) Suba, D.; Urbanyi, Z.; Salgo, A. *J. Pharm. Biomed. Anal.* **2015**, *114*, 53−61.
(150) Vanam, R. P.; Schneider, M. A.; Marlow, M. S. *mAbs.* **2015**, *7* (6), 1118−1127.
(151) Shimura, K.; Hoshino, M.; Kamiya, K.; Enomoto, M.; Hisada, S.; Matsumoto, H.; Novotny, M.; Kasai, K. I. *Anal. Chem.* **2013**, *85*, 1705−1710.
(152) Hühner, J.; Lämmerhofer, M.; Neusüß, C. *Electrophoresis* **2015**, *36*, 2670.
(153) Dada, O. O.; Jaya, N.; Valliere-Douglass, J.; Salas-Solano, O. *Electrophoresis* **2015**, *36*, 2695.
(154) Kinoshita, M.; Nakatsuji, Y.; Suzuki, S.; Hayakawa, T.; Kakehi, K. *J. Chromatogr. A* **2013**, *1309*, 76−83.
(155) Le, M. E.; Vizel, A.; Hutterer, K. M. *Electrophoresis* **2013**, *34*, 1369−1374.
(156) Shi, Y.; Li, Z.; Lin, J. *Anal. Methods* **2012**, *4*, 1637−1642.
(157) Cianciulli, C.; Hahne, T.; Watzig, H. *Electrophoresis* **2012**, *33*, 3276−3280.
(158) Yagi, Y.; Kakehi, K.; Hayakawa, T.; Suzuki, S. *Anal. Sci.* **2014**, *30*, 483−488.
(159) Szekrényes, Á.; Roth, U.; Kerékgyártó, M.; Székely, A.; Kurucz, I.; Kowalewski, K.; Guttman, A. *Anal. Bioanal. Chem.* **2012**, *404* (5), 1485−1494.
(160) Szekrényes, Á.; Park, S. S.; Santos, M.; Lew, C.; Jones, A.; Haxo, T.; Kimzey, M.; Pourkavesh, S.; Szabo, S.; Sosic, Z.; Feng, P.; Varadi, C.; de l'Escaille, F.; Falmagne, J. B.; Seiwal, P.; Niedringhaus, T.; Michels, D.; Freckleton, G.; Hamm, M.; Manuilov, A.; Schwartz, M.; Luo, J. K.; Van Dyck, J.; Leung, P. K.; Olajos, M.; Gu, Y.; Gao, K.; Wang, W.; Wegstein, J.; Tep, S.; Guttman, A. *mAbs* **2015**, 00.
(161) Szigeti, M.; Lew, C.; Roby, K.; Guttman, A. *J. Lab. Autom.* **2015**, 2211068215608767.
(162) Mittermayr, S.; Bones, J.; Guttman, A. *Anal. Chem.* **2013**, *85* (9), 4228−4238.
(163) Hamm, M.; Wang, Y.; Rustandi, R. R. *Pharmaceuticals* **2013**, *6*, 393−406.
(164) Reusch, D.; Haberger, M.; Kailich, T.; Heidenreich, A. K.; Kampe, M.; Bulau, P.; Wuhrer, M. *mAbs* **2014**, *6* (1), 185−196.
(165) Kerékgyártó, M.; Guttman, A. *Electrophoresis* **2014**, *35* (15), 2222−2228.
(166) Jarvas, G.; Szigeti, M.; Guttman, A. *Electrophoresis* **2015**, DOI: 10.1002/elps.201500397.
(167) Henninot, A.; Terrier, A.; Charton, J.; Urbain, R.; Fontayne, A.; Deprez, B.; Beghyn, T. *Anal. Biochem.* **2015**, *491*, 52−54.
(168) Spahr, C.; Shi, S. D. H.; Lu, H. S. *mAbs* **2014**, *6* (4), 904−914.
(169) Zhang, T.; Huang, Y.; Chamberlain, S.; Romeo, T.; Zhu-Shimoni, J.; Hewitt, D.; Zhu, M.; Katta, V.; Mauger, B.; Kao, Y. H. *mAbs* **2012**, *4* (6), 694−700.
(170) Scott, R. A.; Rogers, R.; Balland, A.; Brady, L. J. *mAbs* **2014**, *6* (6), 1453−1463.
(171) Woods, R. J.; Xie, M. H.; Von Kreudenstein, T. S.; Ng, G. Y.; Dixit, S. B. *mAbs* **2013**, *5* (5), 711−722.
(172) Macchi, F. D.; Yang, F.; Li, C.; Wang, C.; Dang, A. N.; Marhoul, J. C.; Zhang, H. M.; Tully, T.; Liu, H.; Yu, X. C.; Michels, D. A. *Anal. Chem.* **2015**, *87*, 10475−10482.
(173) Valliere-Douglass, J. F.; Hengel, S. M.; Pan, L. Y. *Mol. Pharmaceutics* **2015**, *12*, 1774−1783.
(174) Chen, J.; Yin, S.; Wu, Y.; Ouyang, J. *Anal. Chem.* **2013**, *85*, 1699−1704.
(175) Rosati, S.; van den Bremer, E. T. J.; Schuurman, J.; Parren, P. W. H. I.; Kamerling, J. P.; Heck, A. J. R. *mAbs* **2013**, *5* (6), 917−924.
(176) Marcoux, J.; Champion, T.; Colas, O.; Wagner-Rousset, E.; Corvaïa, N.; Van Dorsselaer, A.; Beck, A.; Cianférani, S. *Protein Sci.* **2015**, *24*, 1210−1223.
(177) Huang, R. Y.; Deyanova, E. G.; Passmore, D.; Rangan, V.; Deshpande, S.; Tymiak, A. A.; Chen, G. *J. Am. Soc. Mass Spectrom.* **2015**, *26* (10), 1791−1794.
(178) Wiggins, B.; Liu-Shin, L.; Yamaguchi, H.; Ratnaswamy, G. *J. Pharm. Sci.* **2015**, *104* (4), 1362−1372.
(179) Rosati, S.; Yang, Y.; Barendregt, A.; Heck, A. J. *Nat. Protoc.* **2014**, *9* (4), 967−976.
(180) Thompson, N. J.; Rosati, S.; Heck, A. J. R. *Methods* **2014**, *65* (1), 11−17.
(181) Thompson, N. J.; Hendriks, L. J. A.; de Kruif, J.; Throsby, M.; Heck, A. J. R. *mAbs* **2014**, *6* (1), 197−203.
(182) Haberger, M.; Heidenreich, A. K.; Schlothauer, T.; Hook, M.; Gassner, J.; Bomans, K.; Yegres, M.; Zwick, A.; Zimmermann, B.; Wegele, H.; Bonnington, L.; Reusch, D.; Bulau, P. *mAbs* **2015**, *7* (5), 891−900.
(183) Debaene, F.; Wagner-Rousset, E.; Colas, O.; Ayoub, D.; Corvaïa, N.; Van Dorsselaer, A.; Beck, A.; Cianférani, S. *Anal. Chem.* **2013**, *85*, 9785−9792.

DOI: 10.1021/acs.analchem.5b04561
Anal. Chem. 2016, 88, 480−507

(184) Jones, L. M.; Zhang, H.; Cui, W.; Kumar, S.; Sperry, J. B.; Carroll, J. A.; Gross, M. L. *J. Am. Soc. Mass Spectrom.* **2013**, *24* (6), 835−845.
(185) Fornelli, L.; Damoc, E.; Thomas, P. M.; Kelleher, N. L.; Aizikov, K.; Denisov, E.; Makarov, A.; Tsybin, Y. O. *Mol. Cell. Proteomics* **2012**, *11*, 1758−1767.
(186) Mao, Y.; Valeja, S. G.; Rouse, J. C.; Hendrickson, C. L.; Marshall, A. G. *Anal. Chem.* **2013**, *85*, 4239−4246.
(187) Zhang, Y.; Cui, W.; Zhang, H.; Dewald, H. D.; Chen, H. *Anal. Chem.* **2012**, *84*, 3838−3842.
(188) Nicolardi, S.; Deelder, A. M.; Palmblad, M.; van der Burgt, Y. E. M. *Anal. Chem.* **2014**, *86*, 5376−5382.
(189) Fornelli, L.; Ayoub, D.; Aizikov, K.; Beck, A.; Tsybin, Y. O. *Anal. Chem.* **2014**, *86*, 3005−3012.
(190) Wang, D.; Wynne, C.; Gu, F.; Becker, C.; Zhao, J.; Mueller, H. M.; Li, H.; Shameem, M.; Liu, Y. H. *Anal. Chem.* **2015**, *87*, 914−921.
(191) Pang, P.; Wang, W.; Reid, G. E.; Hunt, D. F.; Bruening, M. L. *Anal. Chem.* **2015**, *87*, 10942−10949.
(192) Dyachenko, A.; Wang, G.; Belov, M.; Makarov, A.; de Jong, R. N.; van den Bremer, E. T. J.; Parren, P. W. H. I.; Heck, A. J. R. *Anal. Chem.* **2015**, *87*, 6095−6102.
(193) Tian, Y.; Han, L.; Buckner, A. C.; Ruotolo, B. T. *Anal. Chem.* **2015**, *87*, 11509−11515.
(194) Pan, J.; Zhang, S.; Parker, C. E.; Borchers, C.H. J. *J. Am. Chem. Soc.* **2014**, *136* (37), 13065−13071.
(195) Pan, J.; Zhang, S.; Chou, A.; Hardie, D. B.; Borchers, C. H. *Anal. Chem.* **2015**, *87*, 5884−5890.
(196) Macht, M. *TrAC, Trends Anal. Chem.* **2013**, *48*, 62−71.
(197) Tran, B. Q.; Barton, C.; Feng, J.; Sandjong, A.; Yoon, S. H.; Awasthi, S.; Liang, T.; Khan, M. M.; Kilgour, D. P. A.; Goodlett, D. R.; Goo, Y. A. *J. Proteomics* **2015**, DOI: 10.1016/j.jprot.2015.10.021.
(198) Srzentic, K.; Fornelli, L.; Laskay, U. A.; Monod, M.; Beck, A.; Ayoub, D.; Tsybin, Y. O. *Anal. Chem.* **2014**, *86*, 9945−9953.
(199) Chen, S. L.; Wu, S. L.; Huang, L. J.; Huang, J. B.; Chen, S. H. *J. Pharm. Biomed. Anal.* **2013**, *80*, 126−135.
(200) Haberger, M.; Bomans, K.; Diepold, K.; Hook, M.; Gassner, J.; Schlothauer, T.; Zwick, A.; Spick, C.; Kepert, J. F.; Hienz, B.; Wiedmann, M.; Beck, H.; Metzger, P.; Molhoj, M.; Knoblich, C.; Grauschopf, U.; Reusch, D. *mAbs* **2014**, *6* (2), 327−339.
(201) Wang, W.; Meeler, A. R.; Bergerud, L. T.; Hesselberg, M.; Byrne, M.; Wu, Z. *Int. J. Mass Spectrom.* **2012**, *312*, 107−113.
(202) Zhang, Y. T.; Hu, J.; Pace, A. L.; Wong, R.; Wang, Y. J.; Kao, Y. H. *J. Chromatogr. B: Anal. Technol. Biomed. Life Sci.* **2014**, *965*, 65−71.
(203) Liu, H.; Ponniah, G.; Neill, A.; Patel, R.; Andrien, B. *Anal. Chem.* **2013**, *85*, 11705−11709.
(204) Wang, S.; Kaltashov, I. A. *Anal. Chem.* **2013**, *85*, 6446−6452.
(205) Shah, B.; Jiang, X. G.; Chen, L.; Zhang, Z. *J. Am. Soc. Mass Spectrom.* **2014**, *25* (6), 999−1011.
(206) Li, C.; Rossomando, A.; Wu, S. L.; Karger, B. L. *mAbs* **2013**, *5* (4), 565−575.
(207) Falck, D.; Jansen, B. C.; Plomp, R.; Reusch, D.; Haberger, M.; Wuhrer, M. *J. Proteome Res.* **2015**, *14* (9), 4019−4028.
(208) Zhu, Z.; Su, X.; Clark, D. F.; Go, E. P.; Desaire, H. *Anal. Chem.* **2013**, *85*, 8403−8411.
(209) Wen, D.; Foley, S. F.; Hronowski, X. L.; Gu, S.; Meier, W. *Anal. Chem.* **2013**, *85*, 4805−48122.
(210) Chumsae, C.; Gifford, K.; Lian, W.; Liu, H.; Radziejewski, C. H.; Zhou, Z. S. *Anal. Chem.* **2013**, *85*, 11401−11409.
(211) Chumsae, C.; Zhou, L. L.; Shen, Y.; Wohlgemuth, J.; Fung, E.; Burton, R.; Radziejewski, C.; Zhou, Z. S. *Anal. Chem.* **2014**, *86*, 8932−8936.
(212) Chumsae, C.; Hossler, P.; Raharimampionona; Zhou, Y.; McDermott, S.; Racicot, C.; Radziejewski, C.; Zhou, Z. S. *Anal. Chem.* **2015**, *87*, 7529−7534.
(213) Li, Y.; Polozova, A.; Gruia, F.; Feng, J. *Anal. Chem.* **2014**, *86*, 6850−6857.
(214) Yang, Y.; Stella, C.; Wang, W.; Schöneich, C.; Gennaro, L. *Anal. Chem.* **2014**, *86*, 4799−4806.
(215) Li, X.; Wang, F.; Xu, W.; May, K.; Richardson, D.; Liu, H. *Anal. Biochem.* **2013**, *436*, 93−100.
(216) Ni, W.; Lin, M.; Salinas, P.; Savickas, P.; Karger, B. L.; Wu, S. L. *J. Am. Soc. Mass Spectrom.* **2013**, *24* (1), 125−133.
(217) Zhang, Y.; Bailey, R.; Nightlinger, N.; Gillespie, A.; Balland, A.; Rogers, R. *J. Chromatogr. B: Anal. Technol. Biomed. Life Sci.* **2015**, *997*, 30−37.
(218) Zhang, A.; Fang, J.; Chou, R. Y.; Bondarenko, P. V.; Zhang, Z. *Biochemistry* **2015**, *54* (10), 1956−1962.
(219) Fu, J.; Bongers, J.; Tao, L.; Huang, D.; Ludwig, R.; Huang, Y.; Qian, Y.; Basch, J.; Goldstein, J.; Krishnan, R.; You, L.; Li, Z. J.; Russell, R. J. *J. Chromatogr. B: Anal. Technol. Biomed. Life Sci.* **2012**, *908*, 1−8.
(220) Brady, L. J.; Scott, R. A.; Balland, A. *Anal. Bioanal. Chem.* **2015**, *407*, 3851−3860.
(221) Ayoub, D.; Bertaccini, D.; Diemer, H.; Wagner-Rousset, E.; Colas, O.; Cianférani; Van Dorsselaer, A.; Beck, A.; Schaeffer-Reiss, C. *Anal. Chem.* **2015**, *87*, 3784−3790.
(222) Janin-Bussat, M. C.; Dillenbourg, M.; Corvaia, N.; Beck, A.; Hamour, C. K. *J. Chromatogr. B: Anal. Technol. Biomed. Life Sci.* **2015**, *981*−*982*, 9−13.
(223) Gautier, V.; Boumeester, A. J.; Lössl, P.; Heck, A. J. R. *Proteomics* **2015**, *15*, 2756−2765.
(224) Rogers, R. S.; Nightlinger, N. S.; Livingston, B.; Campbell, P.; Bailey, R.; Balland, A. *mAbs* **2015**, *7* (5), 881−890.
(225) Zhou, M.; Gucinski, A. C.; Boyne, M. T. *mAbs* **2015**, *7* (6), 1104−1117.
(226) Pirrone, G. F.; Iacob, R. E.; Engen, J. R. *Anal. Chem.* **2015**, *87*, 99−118.
(227) Tang, L.; Sundaram, S.; Zhang, J.; Carlson, P.; Matathia, A.; Parekh, B.; Zhou, Q.; Hsieh, M. C. *mAbs* **2013**, *5* (1), 114−125.
(228) Zhang, S.; Bartkowiak, L.; Nabiswa, B.; Mishra, P.; Fann, J.; Ouellette, D.; Correia, I.; Regier, D.; Liu. *J. Biotechnol. Prog.* **2015**, *31* (4), 1077−1085.
(229) Pan, L. Y.; Salas-Solano, O.; Valliere-Douglass, J. F. *Anal. Chem.* **2014**, *86*, 2657−2664.
(230) Pan, L. Y.; Salas-Solano, O.; Valliere-Douglass, J. F. *Anal. Chem.* **2015**, *87*, 5669−5676.
(231) Iacob, R. E.; Bou-Assaf, G. M.; Makowski, L.; Engen, J. R.; Berkowitz, Z. A.; Houde, D. *J. Pharm. Sci.* **2013**, *102* (12), 4315−4329.
(232) Obungu, V. H.; Gelfanova, V.; Huang, L. *Methods Mol. Biol.* **2013**, *988*, 291−302.
(233) Mysling, S.; Salbo, R.; Ploug, M.; Jorgenson, T. J. D. *Anal. Chem.* **2014**, *86*, 340−345.
(234) Trabjerg, E.; Jakobsen, R. U.; Mysling, S.; Christensen, S.; Jorgenson, T. J. D.; Rand, K. D. *Anal. Chem.* **2015**, *87*, 8880−8888.
(235) Kaur, P.; Tomechko, S. E.; Kiselar, J.; Shi, W.; Deperalta, G.; Wecksler, A. T.; Gokulrangan, G.; Ling, V.; Chance, M. R. *mAbs* **2015**, *7* (3), 540−552.
(236) Deperalta, G.; Alvarez, M.; Bechtel, C.; Dong, K.; McDonald, R.; Ling, V. *mAbs* **2013**, *5* (1), 86−101.
(237) Yan, Y.; Chen, G.; Wei, H.; Huang, R. Y.; Mo, J.; Rempel, D. L.; Tymiak, A. A.; Gross, M. L. *J. Am. Soc. Mass Spectrom.* **2014**, *25* (12), 2084−2092.
(238) Dotz, V.; Haselberg, R.; Shubhakar, A.; Kozak, R. P.; Falck, D.; Rombouts, Y.; Reusch, D.; Somsen, G. W.; Fernandes, D. L.; Wurher, M. *TrAC, Trends Anal. Chem.* **2015**, *73*, 1−9.
(239) Reiding, K. R.; Blank, D.; Kuijper, D. M.; Deelder, A. M.; Wuhrer, M. *Anal. Chem.* **2014**, *86*, 5784−5793.
(240) Echeverria, B.; Etxebarria, J.; Ruiz, N.; Hernandez, A.; Calvo, J.; Haberger, M.; Reusch, D.; Reichardt, N. C. *Anal. Chem.* **2015**, *87*, 11460−11467.
(241) Wang, Y.; Santos, M.; Guttman, A. *J. Sep. Sci.* **2013**, *36*, 2862−2867.
(242) Doneanu, C. E.; Anderson, M.; Williams, B. J.; Lauber, M. A.; Chakraborty, A.; Chen, W. *Anal. Chem.* **2015**, *87* (20), 10283−10291.
(243) Zhu, G.; Sun, L.; Heidbrink-Thompson, J.; Kuntumalla, S.; Lin, H. Y.; Larkin, C. J.; Iv, J. B.; Dovichi, N. J. *Electrophoresis* **2015**, DOI: 10.1002/elps.201500301.

DOI: 10.1021/acs.analchem.5b04561
Anal. Chem. 2016, 88, 480−507

(244) Sandra, K.; Mortier, K.; Jorge, L.; Perez, L. C.; Sandra, P.; Priem, S.; Poelmans, S.; Bouche, M. P. *Bioanalysis* **2014**, *6* (9), 1201−1213.
(245) Hengel, S. M.; Sanderson, R.; Valliere-Douglass, J.; Nicholas, N.; Leiske, C.; Alley, S. C. *Anal. Chem.* **2014**, *86* (7), 3420−3425.
(246) Kaur, S.; Xu, K.; Saad, O. M.; Dere, R. C.; Carrasco-Triguero, M. *Bioanalysis* **2013**, *5* (2), 201−226.

DOI: 10.1021/acs.analchem.5b04561
Anal. Chem. 2016, 88, 480−507